NATIONAL ADVISORY COMMITTEE FOR AERONAUTICS

TECHNICAL NOTE 4328

STUDY OF HYDROGEN EMBRITTLEMENT OF IRON BY INTERNAL-FRICTION METHODS

By R. E. Maringer, E. B. Swetnam, L. L. Marsh, and G. K. Manning
Battelle Memorial Institute

Washington
September 1958

NATIONAL ADVISORY COMMITTEE FOR AERONAUTICS

TECHNICAL NOTE 4328

STUDY OF HYDROGEN EMBRITTLEMENT OF IRON BY INTERNAL-FRICTION METHODS

By R. E. Maringer, E. B. Swetnam,
L. L. Marsh, and G. K. Manning

SUMMARY

The effects of electrolytic charging on the properties of relatively pure iron and tempered 4340 steel were investigated metallographically and by observing internal-friction behavior from -196° to 430° C.

Electrolytic charging caused severe structural damage to both iron and steel, consisting of blisters and internal cracks. In iron, the cracks appeared to initiate at grain boundaries and spread in a transgranular fashion. Removal of carbon by a wet-hydrogen anneal resulted in a strictly intergranular cracking. Reverse-bend testing was used to demonstrate the hydrogen embrittlement of these materials.

The internal friction of recrystallized iron above room temperature was strongly dependent on amplitude, apparently because of the stress-induced motion of magnetic domain boundaries. This damping showed a marked decrease after the addition of hydrogen, due to the structural damage. Below room temperature, both iron and steel showed internal-friction peaks between -150° and -120° C; the nature of these peaks indicated that they are the result of hydrogen interaction with moving dislocations.

The effects of an alternating- or direct-current magnetic field on internal friction are discussed in relation to anomalous internal-friction behavior.

INTRODUCTION

The detrimental effects produced by hydrogen on the mechanical properties of iron and steel have been recognized for a number of years. Hydrogen, after entering the metal, as during a plating or pickling process or by reactions that take place during melting and forming, renders the metal brittle under certain conditions of stress, strain, and temperature. A specimen of hydrogen-bearing steel will, for example, often

fracture under a static load that is only a fraction of its ultimate tensile strength, provided sufficient time is allowed. Inquiring, then, into the nature and environment of the hydrogen atom once it has gained entry into the material in question is of importance.

There has been a considerable amount of work done on the iron-hydrogen system. From this work, hydrogen appears to have a number of sites into which it can settle:

(1) It can go into solution as an interstitial.

(2) It can form an atmosphere in the strained area around a dislocation.

(3) It can go into the disordered regions of grain and subboundaries.

(4) It can collect in internal defects, such as holes, cracks, or inclusions.

In addition to its measured solid solubility (ref. 1), there is other evidence that hydrogen goes into interstitial solid solution. For example, accounting for some of the observed diffusion and permeation data is difficult unless hydrogen is assumed to be in solution. Edwards (ref. 2) and Smithells and Ransley (ref. 3) have demonstrated that grain boundaries have little effect on the diffusion coefficient of hydrogen in iron, so that the bulk of the diffusion must be taking place through the lattice. Moreover, Weiner and Gensamer (ref. 4) have recently reported an internal-friction peak at low temperatures that they interpret to be caused by the stress-induced diffusion of interstitial hydrogen.

There are a number of data indicating that hydrogen segregates into the strained areas around dislocations. Chaudron and his co-workers (refs. 5 and 6) have reported that electrolytic charging with hydrogen and subsequent discharging allowed a mosaic structure to be observed at high magnification in iron single crystals. This result was interpreted to mean that the hydrogen had settled into the mosaic boundaries, which are dislocation arrays, and after repeated charging had opened up these boundaries to the point where they became metallographically visible. X-ray results confirmed the existence of a substructure. However, these results are open to the alternative interpretation of polygonization resulting from charge-induced deformation. Zapffe and Sims (ref. 7) used a similar interpretation of hydrogen-weakened mosaic boundaries to explain the bright appearance of hydrogen-embrittled fracture surfaces.

Recent experiments by Rogers (refs. 8 and 9) are probably more to the point. He charged a 1020 steel with hydrogen and demonstrated a discontinuous yielding that did not occur in uncharged steels. In terms of

the dislocation theory, this means that clouds of hydrogen atoms had formed around the dislocations present. Zapffe (ref. 10) covered the surface of a hydrogen-charged sample with an oil film and observed, under a microscope, the evolution of gas along slip lines and Neumann bands.

There is some evidence that hydrogen is accommodated in grain boundaries, even though the lack of grain-size effects in diffusion studies suggests that hydrogen does not pass through the boundaries preferentially. Bhat (ref. 11) has shown that grain size markedly affects the time lapse between the initiation of a permeability test and the establishment of a steady state of diffusion. The time increases as the grain-boundary area increases and seems to indicate a high solubility of hydrogen in grain boundaries. Some work of de Kazinczy (refs. 12 and 13) showing crack initiation at grain boundaries also suggests the preference of hydrogen for grain boundaries.

There is a great deal of evidence that hydrogen diffuses to holes and cracks in specimens. Once in these holes, the hydrogen atoms can associate to the molecular form that is presumably nondiffusible. Hence, hydrogen can be fed into voids without building up an effective back pressure. According to de Kazinczy, this may result in pressures of over 40,000 atmospheres in the void. Perhaps the most dramatic illustration of this was an experiment by Bridgman (ref. 14). He electrolytically charged a hollow steel cylinder from the outside and observed the internal pressure to reach 9,000 atmospheres (130,000 psi). Such pressures obviously could cause severe structural damage in a specimen.

The purpose of this investigation was to study the nature and environment of hydrogen in iron, particularly by means of internal-friction measurements.

This investigation was carried out at the Battelle Memorial Institute under the sponsorship and with the financial assistance of the National Advisory Committee for Aeronautics.

The authors wish to thank Mr. C. R. Simcoe for many interesting discussions on the subject matter and Mr. P. R. Held for his careful performance of much of the experimental work.

EQUIPMENT

Internal-friction measurements were made in torsional pendulums patterned after that of Kê (ref. 15). The pendulums consisted of a rigid upper grip, a wire specimen, and a free-swinging lower grip supporting an inertia bar. A concave galvanometer mirror on the lower grip reflected the image of a hairline or a slit to a ground-glass scale several

meters distant. Measurements were made by observing the time required for the amplitude of vibration, as observed on the ground-glass scale, to decay to some fraction of the original amplitude. Internal-friction values were computed from the following relation:

$$Q^{-1} = \frac{\log_e n}{\pi f t}$$

where t is the time in seconds required for the amplitude to decrease to 1/nth of its original amplitude, and f is the frequency of oscillation in cycles per second.

One torsional pendulum was constructed to permit measurements of internal friction to be made during charging with hydrogen. The apparatus is shown schematically in figure 1. Tank hydrogen was fed into the apparatus through a glass capillary while the system was being continuously evacuated. A manostat between the vacuum pump and the system maintained the hydrogen atmosphere at 3,000 to 4,000 microns of mercury pressure. A coil of copper tubing surrounded the specimen and formed the anode. The wire specimen itself formed the cathode. When direct-current potential of approximately 350 volts was applied, the hydrogen was ionized and produced the glow discharge. The current flow varied from 15 to 30 milliamperes. The ions were then attracted by their charge to the cathode. In some of the later experiments, a coil comprising 1,000 turns per inch was wound to fit around the upper glass tube. Currents up to 250 milliamperes in this coil served to magnetize the specimen and eliminate damping losses due to magnetomechanical effects.

Electrolytic charging was carried out by using the wire specimen as the cathode and a platium wire coil as the anode. The electrolyte consisted of a solution (by volume) of 4 percent sulfuric acid poisoned by the addition of 6 drops per liter of a solution of 2 grams of yellow phosphorus in 40 cubic centimeters of carbon disulfide. Unless otherwise stated, all specimens were first electropolished and then charged at a current density of 14.5 milliamperes per square inch at about 2.6 volts.

MATERIALS

The materials used in this investigation were a commercially available, vacuum-melted high-purity iron known as Ferrovac E and a 4340 aircraft-quality steel from the same source. The impurities found in the original ingots are given in table I. This material was received in the form of 3-foot straightened, 0.080-inch-diameter wrought wires.

The Ferrovac E wire was cleaned with alcohol, electropolished, and recrystallized in vacuum for 1 hour at 650° and 890° C. This treatment

produced grain sizes of ASTM 8 and ASTM 2, respectively, and will be referred to hereafter as small- and large-grain specimens. Some of the large-grain specimens were extended 3 percent in tension and annealed at 890° C in vacuum for 3 days. This treatment produced crystals completely traversing the wire diameter, up to 3 or 4 centimeters in length. These specimens will be referred to hereafter as very-large-grain-size specimens.

The specimens of 4340 steel were austenitized at 845° C in vacuum, water-quenched, and then tempered at 252°, 370°, or 495° C. The water quench was moderated somewhat by the fact that specimens were sealed in vacuum in Vycor tubes.

EXPERIMENTAL WORK

Metallographic Observations of Charge-Induced Structural Damage

At the start of this investigation, a number of tests were planned to relate mechanical properties with internal-friction and X-ray diffraction data. However, it became obvious from the very beginning that cathodically charging specimens of iron and steel under the conditions adopted caused a rather significant amount of structural damage. This damage was sufficient to cause changes in the properties to be investigated that could not be attributed directly to hydrogen. It was decided, therefore, to investigate the damage metallographically rather than to pursue the indirect method of observing mechanical properties.

Under normal charging conditions (14.5 ma/sq in. at 2.6 v), specimens of recrystallized Ferrovac E became notably blistered after less than an hour. Blisters formed while the specimen was in the charging bath. The blisters, under the microscope, had the appearance of small hills rising sharply from a flat background. The surfaces of the blisters were covered with many lines, some of which tended to follow the blister contours (fig. 2). Many of the blisters were cracked, as in figure 2. Under high magnification (fig. 3), the lines on the blister surface resemble slip lines.

Figure 3 (particularly fig. 3(a)) shows what appears to be a cellular background. A specimen similar to that used for figure 3, but uncharged, was also examined under the electron microscope to see if this structure existed prior to charging. The surface of the uncharged wire, shown in figure 4, is quite different from that of the charged specimen. Numerous larger boundaries, probably subgrain boundaries, appear, but there is little equivalent to the cellular structure seen in figure 3. The contact of the charged specimens with the electrolyte might account for the difference in surface appearance.

When cut in cross section, charged specimens showed many large crack networks. In the cross section of a blister (fig. 5), a crack network usually appeared directly under the blister, often with a crack leading to the surface at the blister.

When a freshly charged specimen was covered with a heavy oil and observed under the microscope, bubbles sometimes could be observed coming from these cracked blisters. On one occasion, bubbles were seen to form at a crack at a rate of several per second, with the rate apparently undiminished after about 20 minutes. When this specimen was totally immersed in oil, several trains of bubbles could be observed originating at different blisters. Seventeen hours later, trains of bubbles were still observable, but at different blisters.

The obvious interpretation of these observations is that hydrogen, trapped in internal holes, builds up sufficient pressure to open up internal cracks. When this process occurs near the surface, a blister results. By diffusion of hydrogen to these voids during continuous charging, the pressure continues to rise until a crack reaches the surface, relieving the pressure. If this is true, the surface markings on the blisters should be deformation markings.

In order to demonstrate this point, a specimen of large-grain-size Ferrovac E was drilled part way through. The pressure of the small drill caused a bulge to appear on the side of the wire away from the drill. Although it was somewhat larger, this bulge had the appearance, to the naked eye, of a charging blister. Under the microscope, it showed the same deformation markings as were observed on the charging blisters (fig. 6).

Blistering, then, leads directly to surface cracks, but the internal cracks are also of great interest. The cracks shown in figure 5 are transcrystalline. These cracks are, however, much too well developed to show where they began. For shorter charging times (fig. 7), the damage appears to initiate at grain boundaries. For Ferrovac E, 10 minutes was the shortest charge that produced readily observable cracks. The tendency of cracks to follow structure is shown clearly in figure 8, where the specimen is as-drawn Ferrovac E.

The fact that neither grain boundaries nor flow lines are necessary for the production of internal cracks during hydrogen charging is made clear in figure 9, which shows the cross section of a charged single crystal of Ferrovac E. It is interesting to note that almost all cracks shown in the photomicrograph appear to be oriented at approximately 45° or 90° from the vertical; this indicates a distinct orientation dependence of crack propagation.

When specimens of Ferrovac E were annealed for 24 hours in wet hydrogen at 712° C, the nature of the charge-induced damage changed significantly. The wet-hydrogen anneal removed most of the carbon (originally 0.009 weight percent) in the material. This apparently resulted in a weakening of the grain boundaries, for the damage due to hydrogen charging was almost entirely confined to grain boundaries (fig. 10). Specimens that were annealed for 63 hours at 710° C in tank hydrogen that was passed through a DeOxo drier behaved in a similar manner (fig. 11).

Specimens of large-grain-size Ferrovac E - recrystallized, wet-hydrogen annealed, and dry-hydrogen annealed - were analyzed by vacuum fusion and found to contain 0.0168, 0.0176, and 0.167 weight percent oxygen, respectively. This percentage is much higher than the oxygen content of the original ingot, but the difference between specimens is almost insignificant, in agreement with the work of Stanley (ref. 16). Hence, it is believed that little or no oxygen was added or removed during the hydrogen anneals.

These results are similar to those of de Kazinczy (ref. 13), who annealed Armco Iron in wet hydrogen and observed predominantly intergranular cracking due to charging. By annealing his samples in dry hydrogen at a significantly higher temperature (1,350° C), de Kazinczy reduced the oxygen content of his iron. This resulted in cracks that, although they appeared to initiate at grain boundaries, were predominantly transcrystalline.

Charging specimens of tempered 4340 steel also produced severe structural damage. Figure 12 is a photomontage of an area showing the orientation and distribution of the cracks after a 17-hour charge. The arrow points out a crack that apparently coincides with a stringer. In general, the cracks appear to be parallel to the wire axis.

Some 4340 steel specimens contained readily apparent cracks after charging periods as short as 1 hour. Specimens charged 1 hour, however, did not always show cracks, and no cracks at all have been observed in specimens charged less than 1 hour. It might be mentioned here that, as the cracks become smaller, differentiating between cracks and inclusions or structure becomes increasingly difficult.

When charging was permitted to continue for longer than 17 hours, the surface of the steel began to change its appearance. After a charge of 65 hours, tempered 4340 steel was badly attacked and contained holes completely traversing the specimen diameter (fig. 13). The holes are, in general, elongated in the direction of the wire axis.

It is believed that, as in the softer Ferrovac E, hydrogen "precipitates" into voids or microcracks, builds up tremendous pressures, and

causes cracks to form and grow. When these cracks eventually reach the surface, the hydrogen pressure is released, and the acid electrolyte proceeds to enter into the crack and attack the inside surface. An example of the process, "caught in the act," is given in figure 14, which is presented here through the courtesy of Mr. C. R. Simcoe of Battelle.

A number of specimens were tested for embrittlement by reverse bending. A small jig held the specimen, and a 1/4-inch length of the specimen was subjected to 90° bends in opposite directions, with the rate of bending held constant to 180° per second. These data, for Ferrovac E, are plotted in figure 15. Each point represents ten to twelve bend specimens.

Both curves for the recrystallized Ferrovac E specimens seem to show a plateau for short charging times. This plateau is especially interesting in the case of the large-grain-size specimens because, as shown in figure 7, significant structural damage had already occurred after 10 minutes of charging. Yet the large-grain-size specimens remain relatively unembrittled after 10 minutes of charging. The length of the plateau increases as the grain size increases and may be associated with this property. If certain sites along grain boundaries act as nuclei for structural damage, then the number of potential nuclei certainly increases with decreasing grain size.

Figure 16 shows the metallographic appearance of as-drawn Ferrovac E, bend-tested after various charging times. Numerous defects are visible. These defects, or cracks, in most cases appear to follow the flow lines in the metal. At the fractured surface, the jagged appearance also indicates that the fracture occurs more readily along the flow lines or grain boundaries.

Tempered at 370° C, 4340 steel is inherently more brittle than Ferrovac E. This steel shows the effects of charging much more rapidly than Ferrovac E. As the data in figure 17 show, a 1-minute charge cuts the number of bends to fracture to less than 10 percent of the uncharged value.

A series of 4340 steel specimens was charged under standard conditions for 1 minute or for 1 hour and was aged for various times at room temperature in order to observe the return of the original bend properties. While the number of bends to failure was quite consistent for all the specimens from any one sample, there were considerable differences from sample to sample. The results of these tests, shown in figure 18, do suggest, however, that the original bend behavior can be restored, with the time required for restoration increasing with the amount of hydrogen present (charging time).

Internal Friction Above Room Temperature

Internal friction, it will be recalled, is the ability of a material completely isolated from its surroundings to dissipate vibrational energy. Internal friction was observed in the present case by measuring the time required for a torsional pendulum (of which the specimen formed the elastic member) to decrease its amplitude of oscillation by a given amount. Since internal friction is a result of relaxation processes within the specimen itself, this property is extremely sensitive to any internal structural changes that affect these relaxation processes.

Internal-friction - temperature tests, at frequencies between 2 and 3 cycles per second, were therefore run on Ferrovac E specimens from room temperature to 430° C to determine the effects of electrolytic hydrogen charging. Specimens were tested in the as-drawn, small-grain-size, large-grain-size, and very-large-grain-size modifications both before and after electrolytic charging. A second run over the same temperature range was made on each of the specimens to determine the effects of annealing resulting from the first run.

For as-drawn Ferrovac E (fig. 19), the internal friction indicates the presence of a peak near 240° C and then appears to rise continuously with increasing temperature. As a result of the anneal incurred during this test, the internal friction was generally lower on the second run, and the peak at 240° C had disappeared. Charging as-drawn specimens with hydrogen produced no observable changes in the character of the curves; hence, the data for charged specimens are not presented.

The dependence of internal friction on temperature for recrystallized Ferrovac E was significantly different. For each of the three modifications examined, the results were qualitatively the same, but the effects noted increased as the grain size increased. Hence, only the data for the very-large-grain size are presented (fig. 20).

In each of the specimen modifications there is a peak at 45° to 60° C. This peak has been reported many times previously (refs. 17 and 18) and is generally conceded to be due to the stress-induced diffusion of carbon in interstitial solid solution. This peak normally appears at about 46° C at the frequency used, and the variation in the observed peak temperatures seems to be associated with the magnetic domain structure, as will be discussed presently.

In the large- and very-large-grain-size specimens, there appears to be a peak in the vicinity of 175° C, with the peak being somewhat larger in the very-large-grain-size specimen. As far as the authors are aware, this peak has not been reported previously, and its identity is unknown. Since the magnitude of this peak increased as the grain size increased, the peak may represent a relaxation process for an element normally found

in the grain boundaries. Certain empirical relations suggest that the peak may be due to interstitial boron, of which less than 0.0006 weight percent is present. This possibility is discussed in more detail later.

At still higher temperatures, about 250° to 270° C in the large- and very-large-grain-size specimens, a third peak was observed. A peak of this type was originally reported by Kê (ref. 15) and subsequently examined in more detail by Köster, Bangert, and Hahn (ref. 19). These authors believe that the internal-friction peak results from the interaction of carbon atoms with moving dislocations. A carbon atom in the stress field of an edge dislocation tends to anchor that dislocation. When a stress is applied to the dislocation, it tends to move away from the carbon atom and, in so doing, exerts a force on the atom. For an alternating stress, such as exists in the torsional pendulum, the work expended in moving the carbon atom to and fro results in an energy-loss maximum at a given temperature, or an internal-friction peak.

If this mechanism is correct, the temperature at which this peak occurs is controlled by the diffusion coefficient of carbon in iron or, in other words, by its ability to move along with a moving dislocation. Wert (ref. 17) has determined the diffusion coefficient of carbon in alpha iron to depend upon temperature as:

$$D = 0.02 \exp(-20{,}000/RT) \text{ cm}^2/\text{sec}$$

For an interaction peak near 250° to 300° C, the diffusion coefficient would be near 1 to 5×10^{-10} square centimeter per second. It is interesting that, in the same temperature region in which the carbon interaction peak occurs in alpha iron, a discontinuity is observed in the flow-stress - temperature curves for alpha iron containing carbon and is ascribed to the same mechanism. In other systems, then, where the diffusion coefficient of a given interstitial is not known, it can be estimated from the temperature at which such a discontinuity occurs either in internal-friction or in flow-stress data.

As in the as-drawn specimen, a second internal-friction - temperature test showed that the effective anneal occurring during the first run had lowered the internal friction over the entire temperature range. The interstitial carbon peak in each specimen modification was lowered; this indicated that some of the carbon originally in solid solution had precipitated. The interaction peak, on the other hand, disappeared completely from the very-large-grain-size specimens, while some traces of it remained in the small- and large-grain-size specimens. The anneal resulted in a much greater resolution of the unidentified 175° C peak in both the large- and very-large-grain-size specimens.

The effect of electrolytic hydrogen charging on each of these specimens was to decrease the internal friction over the whole temperature range. The 175° C peak was completely obliterated, and the interaction peak was very strongly depressed. The interaction peak for each modification had approximately the same magnitude as the interaction peak observed in the as-drawn specimen (note difference in ordinate scales between figs. 19 and 20). The relative lack of an effect of hydrogen charging on the damping of as-drawn Ferrovac E and the large effect of charging on recrystallized Ferrovac E, particularly in view of the structural damage resulting from charging, suggest that the changes observed are due to plastic deformation. The as-drawn specimens, already severely deformed, are relatively unaffected by additional structural damage. The damping of recrystallized specimens, however, should tend toward that of the as-drawn specimen as structural damage becomes more severe.

This fact is made more evident in figure 21, where the internal friction is plotted as a function of strain amplitude during testing at room temperature. Again, the amplitude dependence of the damping increased as the grain size increased, with the amplitude dependence of the very-large-grain-size specimen being too high to make reliable measurements in the present apparatus.

Amplitude-dependent internal friction has been frequently observed. Nowick (ref. 20) has described a process, which he calls "static hysteresis," by which this might occur. If a permanent residual strain remains after the removal of the stress, and a reverse stress is required to return the strain to zero, a hysteresis loop will result even though this relaxation is essentially independent of time. At low temperatures, this process could involve the redistribution of dislocations. Where dislocations were sufficiently anchored by impurities, grain boundaries, or other imperfections, static hysteresis (amplitude dependence) will be minimized. For these reasons, the foregoing results were originally believed to be the result of moving dislocations and static hysteresis.

However, there is a second type of static hysteresis that Nowick describes as "magnetoelastic static hysteresis." Such losses result in a ferromagnetic material from the stress-induced growth of one magnetic domain at the expense of another.

In the domain theory of magnetism, a ferromagnetic material consists of many randomly oriented domains, each of which contains atoms whose magnetic moments are alined in a specific direction. Because of the random orientation, the net magnetic field is zero. However, when a magnetic field is applied, these domains tend to line up in the direction of the magnetic field, and the specimen becomes magnetized. At the same time, the specimen changes dimensions (magnetostriction). As might be predicted, an applied stress (which changes the dimensions) also results in

an alinement of the magnetic domains. The motion, then, under an alternating stress, can produce a strongly amplitude-dependent internal friction.

In order to eliminate the effects of magnetoelastic static hysteresis, it is necessary only to saturate the specimen magnetically. This process serves to line up the magnetic domains and, provided the applied alternating stress is small, prevents any domain motion under the applied stress.

For this purpose a coil consisting of 1,000 turns per inch was wound to surround the specimen in the internal-friction apparatus shown in figure 1. The results of Cochardt (ref. 21) on Armco Iron indicate that an alternating magnetic current was quite effective in reducing magnetoelastic static hysteresis and that maximum effectiveness was observed between 20 and 200 cycles per second. For convenience, therefore, wall current at 60 cycles per second was passed through the coil. As the current passed through the coil increased, the damping was observed first to rise very high, then gradually to fall to a limiting value which was below that observed in the absence of an applied field. In later work, a direct-current source of two 6-volt automobile batteries in series was used, and the damping was observed to decrease immediately on the application of a current to the coil and to continue to decrease toward a limiting value as the current increased. These results agree with the findings of Misek (ref. 22) on the effects of alternating-current and direct-current fields on the damping of nickel.

The internal friction of large-grain-size Ferrovac E became almost independent of amplitude under a sufficiently large magnetic field; hence, it must be concluded that much of the amplitude dependence previously observed was of magnetoelastic origin.

To observe the effects of the magnetic field on the temperature dependence of the damping, the internal friction of large-grain-size Ferrovac E was measured from -50° to 190° C. These data, for damping with and without a pulsating direct-current magnetic field, are shown as solid lines in figure 22. There is indeed a marked decrease in the overall damping as a result of the magnetic field. Perhaps more significant, however, is the difference in the temperature at which the peaks occur. In the presence of the magnetic field, the peak occurs at 46° C, which is, as stated earlier, where the peak should be expected on the basis of the work of other investigators. In the absence of the magnetic field, the peak occurs near 53° C. Moreover, when the curve obtained with the magnetic field is subtracted from the curve without the magnetic field, the difference shows a rather well-defined peak (fig. 22). While the shape of the difference curve might be altered somewhat, the presence of the peak cannot be explained by an error in temperature measurement. It is

probable that the difference curve is the result of domain motion. If such is the case, there appears to be an interaction between domain boundaries and solute carbon atoms that produces an internal-friction peak similar to the stress-induced interstitial diffusion peak.

Since the carbon content of the specimens used (0.009 weight percent) exceeds the solubility limit below around 600° C (ref. 23), the specimens are supersaturated over the whole temperature range investigated. Some transient internal-friction results observed at lower temperatures were believed to result from this supersaturation. Therefore, some large-grain-size specimens were subjected to hydrogen anneals in order to reduce the carbon content. The temperature dependence of the internal friction of these specimens is plotted in figure 23.

One group of specimens was annealed in wet hydrogen for 24 hours at 710° C. The hydrogen was bubbled through water at about 65° C. Another group of specimens was annealed in tank hydrogen passed through a Deoxo catalytic purifier to reduce the water-vapor content. This treatment was carried on for 63 hours, also at 710° C.

The wet-hydrogen-purified specimens had an internal-friction - temperature curve with no discontinuities. This means that the carbon in solution is less the 0.0001 weight percent. In the dry-hydrogen-purified specimen, traces of the previously discussed peaks exist; this indicates that the amount of carbon left in solid solution is perhaps 0.0001 to 0.0002 weight percent. The wet-hydrogen anneal has, as numerous authors have reported, been more effective in lowering the carbon content.

Internal-friction - temperature curves were also obtained for 4340 steel after various tempering treatments. A second set of similar specimens was then cathodically charged with hydrogen for periods of 16 or more hours, and internal-friction - temperature runs were again made. While different tempers resulted in different damping behavior, the effect of hydrogen on this behavior was negligible. Hence, only the data for the uncharged samples are plotted in figure 24.

The significant characteristic of these curves is the presence of a peak at about 235° C, which decreases in magnitude as the tempering temperature increases. A similar peak has been reported in the Russian literature by Rozin and Finkelshtein (ref. 24). These authors studied a 2520-type steel with 0.30 percent carbon and found a peak at 300° C, which decreased in magnitude as the tempering temperature (below 800° C) increased. They ascribed this peak, by analogy with the interstitial carbon peak, to carbon atoms in solid solution in the retained austenite.

As might be expected from some of the previous discussion, the amplitude dependence was not altered by charging with hydrogen. As the data in figure 25 show, however, the magnitude of the damping was increased slightly, probably as a result of the introduction of the cracks previously discussed.

Utilization of Glow Discharge

The equipment used to introduce hydrogen into iron by means of a glow discharge has been described in the section of this report entitled EQUIPMENT and is illustrated in figure 1. In principle, this method of charging is little different from electrolytic charging from an aqueous electrolyte. Hydrogen is ionized, is attracted to the specimen surface by its charge, and then diffuses into the specimen. The rate of charging does, however, appear to be lower under the conditions adopted. Type-4340 steel charged for $1\frac{1}{2}$ hours by glow discharge fractured after three 90° bends. This is roughly the equivalent of a 10-second charge from an acid electrolyte. Ferrovac E, charged by glow discharge for about 2,000 minutes, showed roughly the same amount of internal damage as a similar specimen charged 10 minutes electrolytically. On this basis, the rate of hydrogen charging by aqueous electrolyte is believed to be perhaps 200 to 500 times faster than that by glow discharge.

A number of experiments at constant temperature were performed by measuring internal friction as a function of the time the specimen was subjected to the glow discharge. The results were very erratic and proved exceedingly difficult to reproduce. When a magnetic field was applied to the specimen, however, the erratic nature of the damping disappeared. Figure 26 shows the temperature dependence of wet-hydrogen-annealed Ferrovac E with and without a magnetic field, and before and after exposure to the gaseous glow discharge. There is an appreciable difference in the damping, even after a 1-hour charge. Assuming the rate of charging is 200 to 500 times slower than in the aqueous electrolyte, this result suggests that the internal friction would be influenced by the amount of hydrogen deposited during a 7- to 18-second electrolytic charge.

These same data indicate the nature of the damping often observed in the absence of a magnetic field. The scatter is high, the data are strongly amplitude dependent, and the data do not appear to be consistent from one stage of the experiment to the next. The data in figure 26 taken without the benefit of the magnetic field show peaks that vary from 20° to -25° C. It is probable that these peaks represent a surface condition to which magnetic domain movement is particularly sensitive. It may be, too, that these peaks are similar in origin to the peak in the difference curve shown in figure 22.

It was originally planned to utilize the glow-discharge technique to observe damping near room temperature during hydrogen charging and to differentiate between damping due to hydrogen-dislocation interaction and permanent hydrogen damage. As becomes clearer during the discussion of the various low-temperature phenomena encountered, any effects observed at or near room temperature must be the result of something other than hydrogen-dislocation interaction, for this interaction is observed at much lower temperatures. To control and maintain the glow discharge at temperatures much below 0° C was found to be impossible; therefore, further study in this direction was discontinued.

Internal Friction Below Room Temperature

The internal friction of these same materials was studied from room temperature to -196° C in order to observe any effects that might be due to the presence of hydrogen. In general, the procedure for mounting charged specimens into the apparatus was the same in all cases. The equipment was precooled with dry ice. The specimen was removed from the charging cell, washed with water and alcohol, air-dried, and introduced into the cold apparatus. Normally the specimen was at -40° to -50° C within 5 minutes of its removal from the charging bath. The apparatus was immediately evacuated, then flushed with a dry helium atmosphere.

Much of the earlier work in this program, particularly in the 0° to -60° C temperature region, was plagued by the occasional appearance of nonreproducible phenomena. These phenomena were, in general, internal-friction peaks whose magnitude, shape, and temperature changed from one measurement to the next, frequently disappeared, and defied all efforts to reproduce them. It was noted that the presence of anomalous internal-friction behavior usually coincided with the appearance of rust on the surface of the wire specimen. The effectiveness of the magnetic field in eliminating similar phenomena (fig. 26) and the apparent connection of these phenomena with surface contamination suggest that the mechanism of energy loss is magnetoelastic and due to surface effects.

An example of the changeable nature of these phenomena is given in figure 27. These curves represent eight successive runs on the same specimen. After each run to a maximum of 0° C, the specimen was allowed to cool back down to dry-ice temperatures. The next morning, the same procedure was repeated. In spite of this, each of the curves is appreciably different.

While the nature of these peaks is not known, it is interesting to note that the narrow shape of the peaks indicates that the relaxation mechanism may involve a unique activation energy. The peaks are, therefore, similar in shape to a stress-induced interstitial diffusion peak.

In view of the "difference" peak shown in figure 22 and its apparent dependence on carbon, it is possible that these peaks represent the "difference" peaks for oxygen or nitrogen or even hydrogen. In any event, it is clear that when iron of sufficiently high purity is used, there are a number of unidentified phenomena observable that can easily complicate a system previously believed to be relatively simple.

At a lower temperature, from -70° to -80° C, a very small peak was often, but not always, observed. Its very small magnitude (ΔQ^{-1} max. ≈ 0.0001 or less) made this peak especially difficult to resolve where the background damping was high; this may partly account for its occasional absence. This peak is unidentified and, to the authors' knowledge, has not been reported previously. The peak temperature is close to the temperature at which carbon dioxide sublimes, and it is understandable that such sublimation (or deposition) might affect the damping of a specimen. Therefore, a steel specimen with a low damping capacity was tested at low temperature in the presence of carbon dioxide. The results observed are shown in figure 28 and are compared with an example of the -70° to -80° C peak. No effect of carbon dioxide was observed on cooling but, on heating through -28.5° C, a sharp maximum was produced. This behavior and the general shapes of the observed damping maximum make it probable that these two peaks do not result from the same cause.

Because of empirical relations to be discussed later, it was believed that the peak observed near -80° C might be that for oxygen in solid solution. While the original aim of this work precluded an involved experimental program to investigate this point, several simple experiments were performed. It was assumed that, if interstitial oxygen were the cause of the peak, the peak magnitude could be increased by quenching specimens from higher temperatures where the solubility of oxygen in iron is higher. Quenching from several temperatures between 400° and 890° C, however, failed to give any consistent results. The internal friction of these same specimens was also measured above room temperature to observe the effects of heat treatment on the peak at 175° C, which possibly could be due to boron in solid solution. Again, the results were inconsistent. It appeared, in fact, that quenching may have suppressed both of these peaks. Unfortunately, these results were obtained prior to the introduction of the magnetic coil of the apparatus, and the high background damping may have obscured any actual changes.

Charging specimens of Ferrovac E and 4340 steel with hydrogen from an aqueous electrolyte produced, as discussed earlier, severe internal structural damage in the form of holes and cracks with their associated plastic deformation. This damage resulted in a general lowering of the internal friction above room temperature, presumably by interfering with the motion of magnetic domain boundaries and dislocations. A similar behavior was observed in the damping below room temperature. Below about

-90° C, however, and under certain conditions, the presence of hydrogen caused more direct effects and resulted in the appearance of at least two internal-friction maximums.

When recrystallized Ferrovac E was electrolytically charged with hydrogen, there was little, if any, indication of an internal-friction peak below -90° C. Charged as-drawn Ferrovac E (which had been at room temperature for perhaps 18 months before charging and testing) did show a small maximum near -130° C. Another specimen of recrystallized Ferrovac E, which had been annealed in wet hydrogen for 1 hour at 710° C, showed a similar peak after a similar charge. This anneal had reduced the carbon in solution to about 0.001 weight percent, as measured by internal friction. However, when the carbon in solution had been reduced by a wet-hydrogen anneal to below 0.0001 weight percent, as measured by internal friction, a well-defined but rather broad peak of appreciable magnitude appeared at -130° C. Aging at room temperature caused the peak to decrease in magnitude and to shift toward lower temperatures (fig. 29). Actually, there appear to be two internal-friction peaks separated in temperature by about 20° C (fig. 30). The higher (-130° C) peak appears first, with the lower (-150° C) peak increasing in magnitude during aging.

Early attempts to study these peaks were hampered by variations in background damping and by a lack of reproducibility. Application of a magnetic field, as previously discussed, lowered the background damping and increased the reproducibility but did not seem to cause any appreciable qualitative difference in the nature of the internal-friction peaks.

The activation energy for the relaxation process controlling the -130° C peak was determined experimentally by observing the shift in the temperature at which the peak occurred for different frequencies of oscillation. The activation energy H was determined from the relation

$$H = R \log_e \frac{f_1}{f_2} \left(\frac{T_2 T_1}{T_1 - T_2} \right)$$

where R is the gas constant, f_1 and f_2 are frequencies of oscillation in cycles per second, and T_1 and T_2 are the peak temperatures in degrees Kelvin. These data are shown in figure 31. The activation energy determined is 7,600 ± 1,000 calories per mole, which is in reasonable agreement with the 9,000 calories per mole predicted by the empirical relationship of Wert and Marx (ref. 25) on the basis of the temperature at which the peak occurs.

The low-temperature internal friction of 4340 steel is also affected by a hydrogen charge. A 1-minute charge produces an appreciable peak at -125° C in as-drawn 4340 steel (fig. 32). A 10-minute charge on the same

material produces a larger peak at the same temperature. However, a 1-minute charge produces no peak in tempered 4340 steel, and charging for a full hour on this material produces a peak of only about half the magnitude of the 1-minute peak in the as-drawn steel.

Tempered 4340 steel that had been charged for 1 hour was aged for various times at room temperature to observe changes in the low-temperature internal friction. This damping was characterized by many, and often abrupt, changes in the internal friction (fig. 32). Aging for 168 hours led to the disappearance of the peak at -125° C and to the appearance of a peak at -80° C. After 227 hours at room temperature, the -80° C peak had almost disappeared, but discontinuities in the data continued.

The appearance of a peak at -80° C on several different tests of steel as well as of Ferrovac E suggests that this peak is real, but an insufficient amount of data exist to state this with any certainty. The abrupt changes in damping that are occasionally observed (as in fig. 32) do not conform to the usual characteristics of an internal-friction peak and are believed to be associated with the spread of internal cracks as a result of the combination of internal hydrogen pressure and the applied external-measuring stress.

Weiner and Gensamer (ref. 4) have reported an internal-friction peak at between -158° and -178° C for a 1020 steel after electrolytic charging or after subjecting the specimen to a high hydrogen pressure at high temperatures. This peak is not immediately present, but it increases in magnitude with aging at room temperature and reaches a maximum height after about 4 days of aging. This increasing magnitude with aging is similar to that observed for the -150° C peak in Ferrovac E, but this behavior was not observed in the same temperature range in tempered 4340 steel.

Weiner and Gensamer believe that their peak near -160° C is due to the interaction of hydrogen atoms with moving dislocations. This interaction peak comes about in the same way as the carbon interaction peak previously discussed. There appears to be good reason to believe that this is the case.

These low-temperature peaks are rather broad - much broader, in fact, than would be expected for a peak controlled by a nearly unique activation energy, such as one normally observes for an interstitial diffusion peak. The effects of carbon in reducing the magnitude of the peak are accounted for most easily if the peak is assumed to be the result of interaction. Carbon then anchors the dislocations so that they cannot move at low temperatures regardless of whether or not hydrogen is present.

In steel, deforming the specimen plastically is necessary before any carbon interaction peak is observed. Relatively free lengths of movable

dislocations must be introduced before the interaction of carbon can be observed. The more rapid appearance of a larger internal-friction peak due to hydrogen in as-drawn 4340 steel, as compared with the tempered steel, implies the same requirement for the present low-temperature peaks.

Weiner and Gensamer also reported a second internal-friction peak at about 50° K, which they have interpreted as due to the stress-induced diffusion of interstitial hydrogen. This point has been plotted along with the diffusion data of Stross and Tompkins (ref. 26), as well as some others, in figure 33. Assuming, as for the carbon interaction peak, that the hydrogen interaction peak occurs when the diffusion coefficient of the interstitial is between 10^{-9} and 10^{-10} square centimeters per second, the observed interaction peak temperatures have been included in the figure at this value of the diffusion coefficient. The agreement is sufficiently good to support the hypothesis that the 50° K peak is due to stress-induced interstitial diffusion, while the peaks above 100° K are due to hydrogen-dislocation interaction.

This hypothesis cannot, of course, be accepted without question. It is, for example, difficult to explain the observation of two interaction peaks in Ferrovac E, while Weiner and Gensamer (ref. 4) report only one in 1020 steel. It is difficult also to explain the differences in the observed temperatures between reference 4 and this report other than to ascribe them to the fact that different purities were involved in the specimens used. There seem, however, to be some discrepancies in the reported carbon-interaction peak temperatures among various authors. Again, different purity materials were used and may account for the differences. No reports of double interaction peaks are known to the authors, although both oxygen and nitrogen produce double interstitial peaks in tantalum.

While these questions are at the present time unanswerable, the width of the observed peaks, their aging behavior, the effects of impurities and deformation on peak behavior, and the agreement of calculated diffusion coefficients from the -130° to -160° C peaks and from the peak of Weiner and Gensamer at 50° K indicate that the proposed hypothesis is correct. That is, the peaks between -130° and -160° C result from the interaction of hydrogen atoms and moving dislocations, while the 50° K peak results from the stress-induced diffusion of interstitial hydrogen. On the basis of this hypothesis, temperature dependence of the diffusion coefficient of hydrogen can be expressed by the relation

$$D = (8\times10^{-3})\exp\left[(-3{,}100 \pm 300)/RT\right] \text{ cm}^2/\text{sec}$$

The uncertainty in the activation energy is a result of the uncertainty of the exact peak temperature near 50° K and can be much more accurately determined when more exact measurements of this peak are available.

Empirical Observations

In the opinion of the authors, interstitial solutes in body-centered-cubic solvents should behave in a qualitatively similar way, and such similarities might be of use in determining the nature of interstitial hydrogen in iron and steel. For this reason, data were collected from the literature concerning the internal friction of interstitial solutes in body-centered-cubic solvents. The data collected involved the systems Fe-N, Fe-C, Ta-O, Ta-C, Ta-N, Nb-O, Nb-C, Nb-N, V-O, and V-N. To these were added, of course, the available data from the system Fe-H.

It was noted that, in most cases, as the Goldschmidt atomic radius of the interstitial solute increased, the temperature of the internal-friction peak caused by that solute in a given solvent increased. There are two exceptions to this: Ta-C and Nb-C. The carbon peak originally reported in tantalum (ref. 27) was later shown to be actually a second oxygen peak (ref. 28). A recent report (ref. 29) indicates that the real carbon peak is very close to, but still at a slightly lower temperature than, the nitrogen peak. The reported carbon peak in niobium occurs near the oxygen peak and may be a case of mistaken identity, as in the case of tantalum.

For alpha iron, when the logarithm of the Goldschmidt atomic radius is plotted against the temperature at which the internal-friction peak corresponding to that solute occurs (using peaks for H, N, and C), the result is approximately a straight line. If the assumption is made that the -80° C and the 175° C peaks are due to oxygen and boron, respectively, these points also fit the same straight line.

The qualitative nature of such a plot is not unreasonable. The peak temperature for a frequency of about 1 cycle per second can be used to calculate (ref. 17) diffusion coefficients from the relation

$$D = \frac{\pi a^2 f}{18}$$

where a is the lattice parameter of the solvent and f is the frequency of oscillation (approx. unity).

Except for the effect of the temperature dependence of the lattice parameter, then, the various peak temperatures represent the temperature at which a particular diffusion coefficient occurs. This suggests that, as the size of the solute atom increases, it becomes increasingly difficult for that atom to make a given lattice jump. The atom must acquire more energy, which in turn demands a higher temperature.

Perhaps a more valid correlation would be obtained by using the activation energy term ΔH of the diffusion equation $D = D_0 \exp(-\Delta H/RT)$, where D_0 is the diffusion constant.

This quantity has been experimentally determined for most of the binary systems under discussion and can be estimated from the relation of Wert and Marx (ref. 25) for the peaks presumably due to oxygen, hydrogen, and boron in alpha iron. For convenience of presentation, these data are presented as the logarithm of the Goldschmidt atomic radius against $\Delta H/T_m$, where T_m is the melting point of the pure solvent (fig. 34). Other plots can be made to demonstrate a similar parallelism. Unfortunately, not enough data exist to substantiate any given method of plotting. Figure 34 serves, however, to demonstrate that there exists a familylike relation in the diffusion characteristics of interstitial solutes in various body-centered-cubic solvents.

A single attempt was made to charge tantalum wire with hydrogen electrolytically and to observe an internal-friction peak due to hydrogen. Tantalum, which was, incidentally, severely embrittled, exhibited a large peak at -80° C. The peak is quite broad and is more likely to be an interaction peak than an interstitial peak. However, as evidenced by a plot of the estimated activation energy in figure 34, the peak fits the correlation presented.

In considering the tentative nature of atomic radii and the normal scatter observed in activation energy determinations, it is surprising that such an empirical relation holds so well. Of interest, too, is the ordinate $\Delta H/T_m$. Dienes (ref. 30) has shown a linear relation to exist between ΔS, which is the entropy of activation, and $\Delta H/T_m$. The relation suggests that the entropy increases as the solute atomic radius increases, and implies that the empirical plot may have some physical significance.

In view of this fact and the internal consistency of the empirical relations, the assumed identities of the -80° C (oxygen) and the +175° C (boron) peaks acquire some strength. Unfortunately, there is little in the literature that might contribute to these assumptions. With respect to boron, Busby and Wells (ref. 31) determined diffusion coefficients in alpha iron at 700°, 751°, and 835° C. These authors stated that the data corresponded to the relation

$$D = 10^6 \exp(-62{,}000/RT) \text{ cm}^2/\text{sec}$$

but emphasized that the sparseness of the data cast considerable doubt on the constants determined.

If the 175° C peak is assumed to be due to interstitial boron, the diffusion coefficient of 175° C can be calculated to be about 3×10^{-16} square centimeters per second. This point, plotted with the data of Busby and Wells (fig. 35), defines a line that conforms to the relation

$$D = 0.2 \exp(-30{,}000/RT) \text{ cm}^2/\text{sec}$$

The value of 0.2 for D_o would be much more in line with what might be expected, since most values for this constant for interstitials in body-centered-cubic lattices lie between 10^{-1} and 10^{-2} (ref. 32).

This interpretation does not agree with that of Leak (ref. 33), who finds an activation energy of 17,500 calories per mole for a small peak, attributed to boron, that occurs near that for carbon in alpha iron. The possibility that boron may be able to enter into either substitutional or interstitial solid solution, or may alter the diffusion characteristics of nitrogen or carbon, may account for these discrepancies. It must be stressed, however, that the identification of the 175° C peak with interstitial boron is purely on an empirical basis, with considerable uncertainty involved, and must therefore be only speculative.

DISCUSSION

From the nature of the observed structural damage caused by hydrogen in iron and steel, it is clear that hydrogen can collect and build up extreme pressures in grain boundaries and in preexisting cracks or flaws. The nature of the structural damage observed in a single crystal of pure iron (fig. 9) suggests, moreover, that neither grain boundaries nor internal flaws are required as crack nuclei. The directionality of the cracks in the single crystal indicates that hydrogen can collect on and spread along preferred crystallographic planes. This behavior might be interpreted as being due to the collection of hydrogen around a dislocation array and the eventual initiation of a crack at this array. The internal-friction data, as interpreted, also support the position that hydrogen collects around and anchors dislocation. The internal-friction data also support the existence of hydrogen in solid solution. On the basis of these observations and conclusions, the character of hydrogen embrittlement can be discussed with at least a limited understanding.

The initiation of a crack in iron or steel containing hydrogen can occur at any site where molecular hydrogen can form, and the crack can continue to grow as long as hydrogen is available to supply the crack with additional pressure. It seems that this should occur independently of any effect that adsorbed hydrogen might have on lowering the surface energy of the crack. The important factors to consider are: (1) The amount of hydrogen contained in the material, and (2) the ability of hydrogen to move in the lattice.

The determination of how much hydrogen might be contained in a specimen is difficult, if the fact that the hydrogen may exist in holes in the gaseous phase as well as in solid solution is considered. At low temperatures, the hydrogen content can vary tremendously. At higher temperatures, the gas trapped in the holes dissociates and diffuses away, so

that the buildup of internal cracks is not observed. Wet- or dry-hydrogen treatment at high temperatures, for example, does not produce structural damage despite long exposure times. At high temperatures the hydrogen content of the material is presumably controlled by the solubility of hydrogen under the particular conditions (hydrogen activity) of exposure to a hydrogen-bearing atmosphere.

When hydrogen is introduced at low temperatures, as during plating or pickling, the solubility of the hydrogen does not limit the amount of hydrogen that can be contained by a given specimen. Not only is the activity of the hydrogen at the entry surface extremely high under these conditions, but the conditions for precipitation in the gaseous phase into holes or voids appear to be at a maximum.

Under these conditions, the amount of hydrogen that can be transferred from the material surface to internal "embryo" cracks is controlled by the permeability of the steel to hydrogen. Permeability is, of course, a function of both solubility and diffusion coefficient.

It would appear reasonable, then, that the embrittlement caused by the introduction of hydrogen at high temperatures should be eased by a reduction in hydrogen solubility, while the embrittlement caused by the introduction of hydrogen at low temperatures should be eased by a reduction of either or both the solubility limits or the diffusion coefficient of hydrogen in iron or steel. This embrittlement possibly might be affected by alloying. Geller and Sun (ref. 34) reported, for example, that silicon additions lowered the permeability of alpha iron toward hydrogen. More recently, Klier, Muvdi, and Sachs (ref. 35 indicated that silicon-bearing steels are less susceptible to hydrogen embrittlement during cadmium plating than similar steels without silicon. Silicon has been shown to reduce the solubility of nitrogen in iron (ref. 36). If the interstitials in iron are as similar in behavior as the empirical correlation presented indicates, silicon additions may well be found to alter hydrogen solubility. Indeed, such an effect is easily postulated to explain the results of Geller and Sun (ref. 34).

The preceding generalities are based upon the assumption that only hydrogen pressure in cracks is responsible for hydrogen embrittlement. In the presence of a continuous supply of hydrogen, cracks might be expected to form and spread. Where an external load is applied to the specimen, the cracks could link together, and the specimen would be expected to fail when its effective cross-sectional area had decreased sufficiently to allow the external load alone to spread the cracks. Such a mechanism would explain many of the delayed failure observations. By this means, explaining the disappearance of embrittlement at low temperatures or at very high strain rates becomes more difficult. To account for this, Petch and Stables (ref. 37) have proposed that hydrogen will

be chemisorbed on the fracture surface of iron and will markedly reduce the surface energy of the iron, so that the energy required to spread the crack is lowered. The rate at which a crack can spread must then be limited by the rate at which hydrogen can reach and be adsorbed on the crack surface. Since either a decrease in temperature or an increase in strain rate would decrease the rate of hydrogen adsorption, this mechanism can readily account for the observed temperature- and strain-rate dependence of hydrogen embrittlement.

It is probable, therefore, that the actual mechanism of hydrogen embrittlement involves the initiation of cracks by the development of high hydrogen pressures, with the spread of these cracks accelerated by a lowering of the surface energy of the fracture surface. Again, a decrease in hydrogen solubility and/or diffusion coefficient by alloying seems to offer a possible means for the alleviation of hydrogen embrittlement.

CONCLUSIONS

An investigation of the hydrogen embrittlement of relatively pure iron and tempered 4340 steel by internal-friction and metallographic observations gave the following results and conclusions:

(1) Electrolytic charging, under the conditions adopted, produces severe structural damage in iron and in 4340 steel even after comparatively short charging times.

(2) Charge-induced damage appears, in part, to nucleate at internal flaws and grain boundaries.

(3) Structural damage can be induced by electrolytic charging in the absence of observable flaws or grain boundaries.

(4) The internal friction of recrystallized iron is particularly sensitive to structural damage produced by hydrogen charging.

(5) The internal friction of iron and steel below room temperature exhibits phenomena resulting from the interaction of hydrogen atoms and moving dislocations.

(6) Much of the anomalous internal-friction behavior observed in pure iron can be accounted for in terms of magnetoelastic energy losses.

Battelle Memorial Institute,
Columbus, Ohio, June 30, 1957.

REFERENCES

1. Anon.: Metals Handbook. ASM, Cleveland (Ohio), 1948, p. 1208.

2. Edwards, C. A.: Pickling; or the Action of Acid Solutions on Mild Steel and the Diffusion of Hydrogen Through the Metal. Jour. Iron and Steel Inst., vol. CX, no. 11, 1924, pp. 9-44; discussion, pp. 45-60.

3. Smithells, C. J., and Ransley, C. E.: The Diffusion of Gases Through Metals. Proc. Roy. Soc. (London), ser. A, vol. 150, no. 869, May 1, 1935, pp. 172-192; discussion, pp. 192-197.

4. Weiner, L. C., and Gensamer, M.: The Effects of Aging and Straining on the Internal Friction of Hydrogen Charged 1020 Steel at Low Temperatures. Acta Metall., vol. 5, no. 12, Dec. 1957, pp. 692-694.

5. Chaudron, G.: Divers modes de fixation de l'hydrogéns par les métaux. Métaux Corrosion-Usure, vols. 229-230, Sept.-Oct. 1944, pp. 92-93.

6. Benard, J.: Etude aux rayons X de la dislocation d'un cristal unique de fer par chargement d'hydrogéne. Métaux Corrosion-Usure, vol. 19, nos. 231-232, Nov.-Dec. 1944, p. 106.

7. Zapffe, C. A., and Sims, C. E.: Hydrogen Embrittlement, Internal Stress and Defects in Steel. Trans. AIME, vol. 145, 1941, pp. 225-261; discussion, pp. 261-271.

8. Rogers, H. C.: A Yield Point in Steel Due to Hydrogen. Acta Metall., vol. 2, Jan. 1954, p. 167.

9. Rogers, H. C.: The Influence of Hydrogen on the Yield Point in Iron. Acta Metall., vol. 4, no. 2, Mar. 1956, pp. 114-117.

10. Zapffe, C. A.: Neumann Bands and the Planar-Pressure Theory of Hydrogen Embrittlement. Jour. Iron and Steel Inst., vol. CLIV, 1946, pp. 123-130.

11. Bhat, U. V.: Diffusion of Hydrogen in Steel. Trans. Indian Institut. Metals, vol. 4, 1950, pp. 279-286; discussion, pp. 287-289.

12. de Kazinczy, F.: Hydrogen Occlusion and Equilibrium Hydrogen Pressure in Steel During Electrolytic Charging. Jernkontorets Annaler, vol. 139, no. 7, 1955, pp. 466-480.

13. de Kazinczy, F.: Formation of Blisters in Iron. Jernkontorets Annaler, vol. 140, no. 5, 1956, pp. 347-359.

14. Bridgman, P. W.: The Physics of High Pressure. G. Bell (London), 1952, pp. 96-97.

15. Kê, Ting-Sui: Anelastic Properties of Iron. Trans. AIME, vol. 176, 1948, pp. 448-474; discussion, pp. 474-476.

16. Stanley, James K.: The Embrittlement of Pure Iron in Wet and Dry Hydrogen. Trans. ASM, vol. 44, 1952, pp. 1097-1106; discussion, pp. 1106-1116.

17. Wert, C. A.: Diffusion Coefficient of C in Alpha-Iron. Phys. Rev., vol. 79, Aug. 15, 1950, pp. 601-605.

18. Dijkstra, L. J.: Elastic Relaxation and Some Other Properties of the Solid Solutions of Carbon and Nitrogen in Iron. Philips Res. Rep., vol. 2, Oct. 1947, pp. 357-381; 399-400.

19. Köster, Werner, Bangert, Lothar, und Hahn, Rolf: Das Dämpfungsverhalten von gerecktem technischem. Archiv f. das Eisenhuttenwesen, Jahrg. 25, Heft 11/12, Nov.-Dec. 1954, pp. 569-578.

20. Nowick, A. S.: Internal Friction in Metals. Vol. 4 of Prog. in Metal Phys., Interscience Publ., Inc., 1953, pp. 1-70.

21. Cochardt, A. W.: Some New Magneto-Mechanical Torsion Experiments. Jour. Appl. Phys., vol. 25, no. 5, May 1954, pp. 670-673.

22. Míšek, Karel: A Magnetic Internal Friction Peak in Nickel under Alternating Magnetic Fields. Acad. Sinica (Peking), vol. 4, 1955, pp. 107-118.

23. Wert, Charles A.: Solid Solubility of Cementite in Alpha Iron. Trans. AIME, vol. 188, Oct. 1950, pp. 1242-1244.

24. Rozin, K. M., and Finkelshtein, B. N.: Study of Phase Transformations by Internal Friction Methods. DC-NSF-TR-143, Nat. Sci. Foundation, AEC (Washington, D. C.), Dec. 1953. (Trans. from Doklady Akad. Nauk SSSR, vol. 91, 1953, pp. 811-812.)

25. Wert, C. A., and Marx, J. A.: A New Method for Determining the Heat of Activation for Relaxation Processes. Acta Metall., vol. 1, Mar. 1953, pp. 113-115.

26. Stross, T. M., and Tompkins, F. C.: The Diffusion Coefficient of Hydrogen in Iron. Jour. Chem. Soc., Feb. 1956, pp. 230-234.

27. Kê, T. S.: Internal Friction in the Interstitial Solid Solutions of C and O in Tantalum. Physical Rev., vol. 74, 1948, pp. 9-15.

28. Powers, R. W.: Internal Friction in Solid Solutions of Tantalum-Oxygen. Acta Metall., vol. 3, 1955, pp. 135-139.

29. Powers, R. W., and Doyle, M. V.: Carbon Tantalum Internal Friction Peak. Jour. Appl. Phys., vol. 28, Mar. 1957, pp. 255-258.

30. Dienes, G. J.: Frequency Factor and Activation Energy for the Volume Diffusion of Metals. Jour. Appl. Phys., vol. 21, no. 11, Nov. 1950, pp. 1189-1192.

31. Busby, P. E., and Wells, C.: Diffusion of Boron in Alpha-Iron. Jour. Metals, vol. 6, no. 9, sec. 1, Sept. 1954, p. 972.

32. Wert, C. A.: The Metallurgical Use of Anelasticity. Modern Res. Techniques in Phys. Metallurgy, ASM (Cleveland), 1953, pp. 225-250.

33. Leak, G. M.: Boron in Iron and Steel. Hardenability and Its Mechanism. Metal Treatment and Drop Forging, vol. 23, no. 124, Jan. 1956, pp. 21-28.

34. Geller, Werner, and Sun, Tak-Ho: Einflub von Legierungszusätzen auf die Wasserstoffdiffusion im Eisen und Beitrag zum System Eisen-Wasserstoff. Archiv f. das Eisenhuttenwesen, Jahrg. 21, Heft 11/12, Nov.-Dec. 1950, pp. 423-430.

35. Klier, E. P., Muvdi, B. B., and Sachs, G.: Design Properties of High-Strength Steels in the Presence of Stress Concentrations and Hydrogen Embrittlement. Pt. 3 - The Response of High-Strength Steels in the Range 180,000-3000,000 PSI to Hydrogen Embrittlement from Cadmium Electroplating. TR 56-395, Summary Rep. Sept. 1955-Aug. 1956, WADC, Mar. 1957. (Contract AF-33(616)-2362.)

36. Rawlings, R.: The Effect of Silicon on the Solubility of Nitrogen in Alpha- and Gamma-Iron. Jour. Iron and Steel Inst., vol. 185, Jan.-Apr. 1957, pp. 441-449.

37. Petch, N. J., and Stables, P.: Delayed Fracture of Metals under Static Load. Nature, vol. 169, May 17, 1952, pp. 842-843.

38. Demarez, Al., Hock, Arthur G., and Meunier, Francis A.: Diffusion of Hydrogen in Mild Steel. Acta Metall., vol. 2, no. 2, Mar. 1954, pp. 214-223.

TABLE I. - IMPURITY CONTENTS OF FERROVAC E IRON AND 4340 STEEL

	Impurity, weight percent													
	C	Mn	O_2	N_2	Si	Ni	Cr	Sn	V	Co	Cu	Al	Pb	Mo
Ferrovac E	0.009	0.001 to 0.003	0.0031	0.0001	0.008 to 0.01	0.001 to 0.003	<0.001	<0.004	<0.002	<0.005	0.001 to 0.003	<0.003	<0.01	
4340 Steel	.38	.72			.24	1.75	.75							0.25

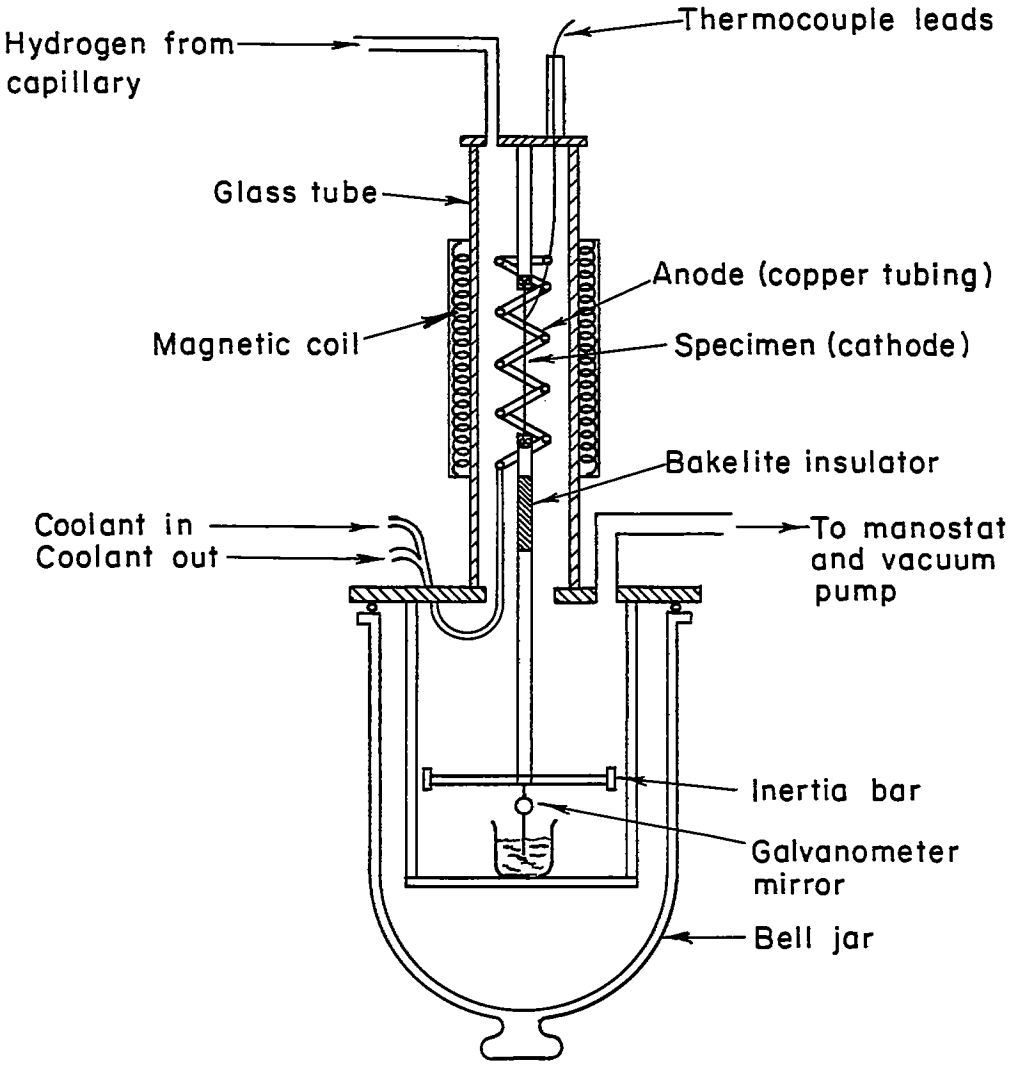

Figure 1. - Glow-discharge internal-friction apparatus.

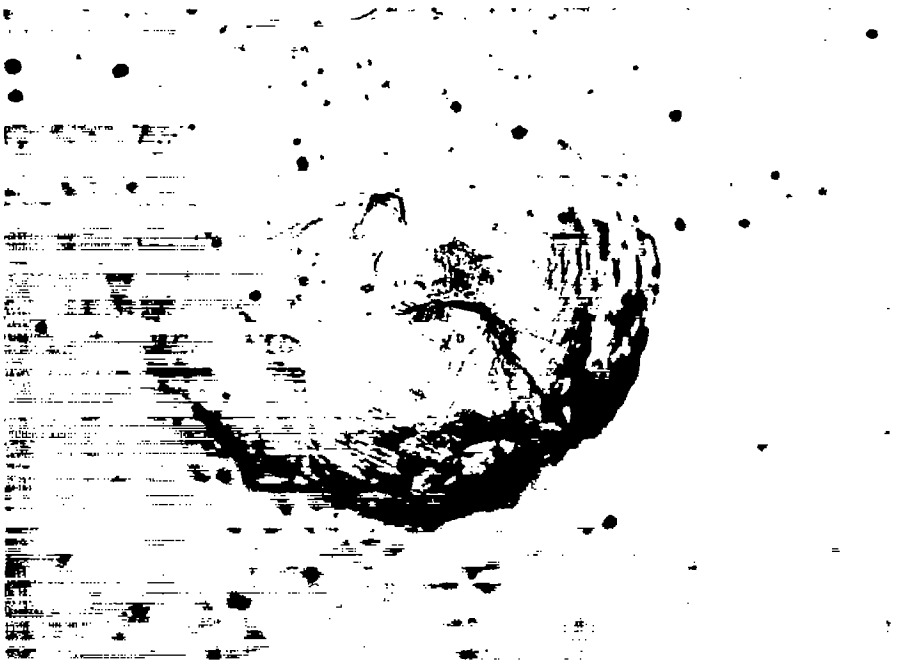

(a) With cracks.

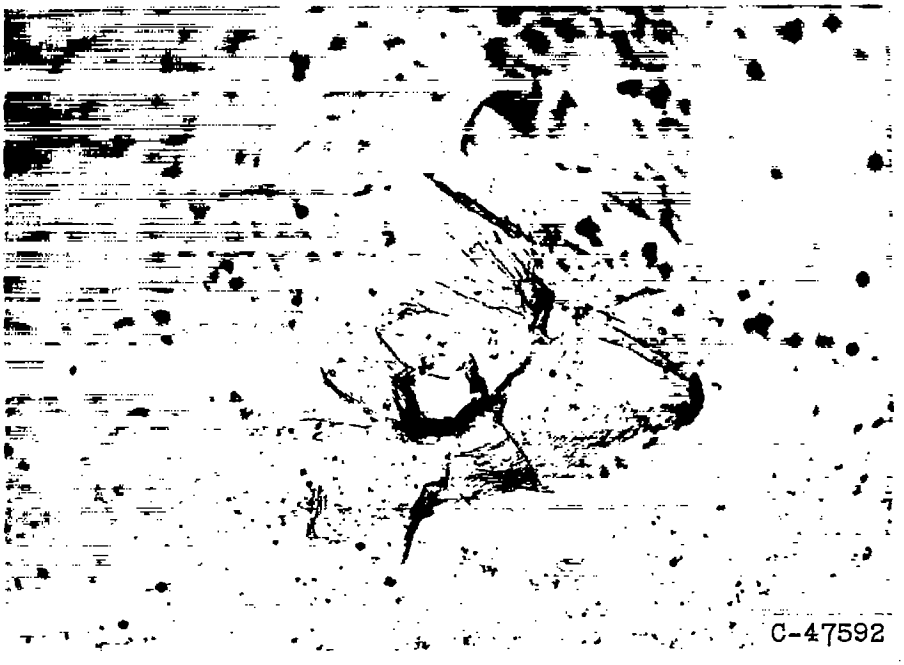

(b) Without cracks.

Figure 2. - Surface blisters on large-grain-size Ferrovac E, charged 3 hours; X250.

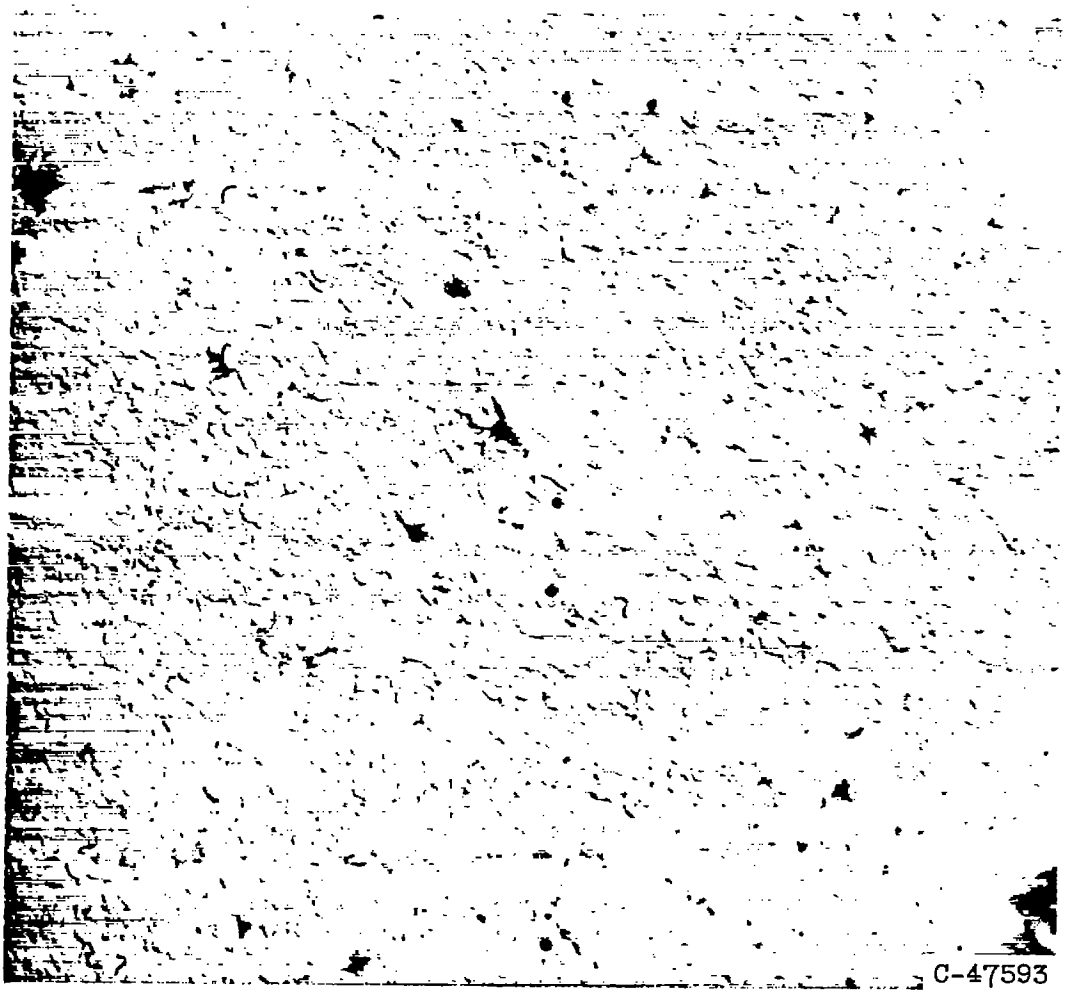

(a) Example 1. (Note cellular-background appearance.)

Figure 3. - Electron micrographs of surface of blister on charged, large-grain-size Ferrovac E. Platinum preshadowed positive silica replica; X10,000.

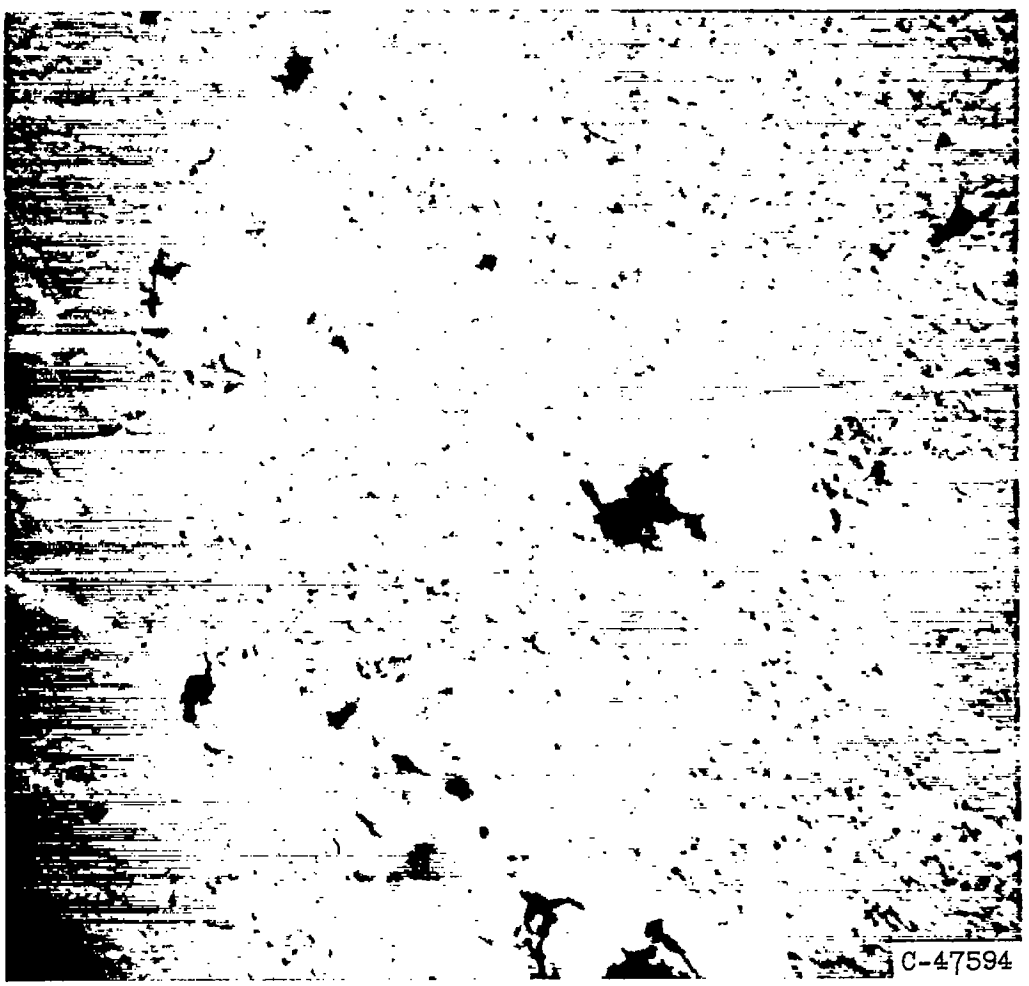

(b) Example 2.

Figure 3. - Concluded.

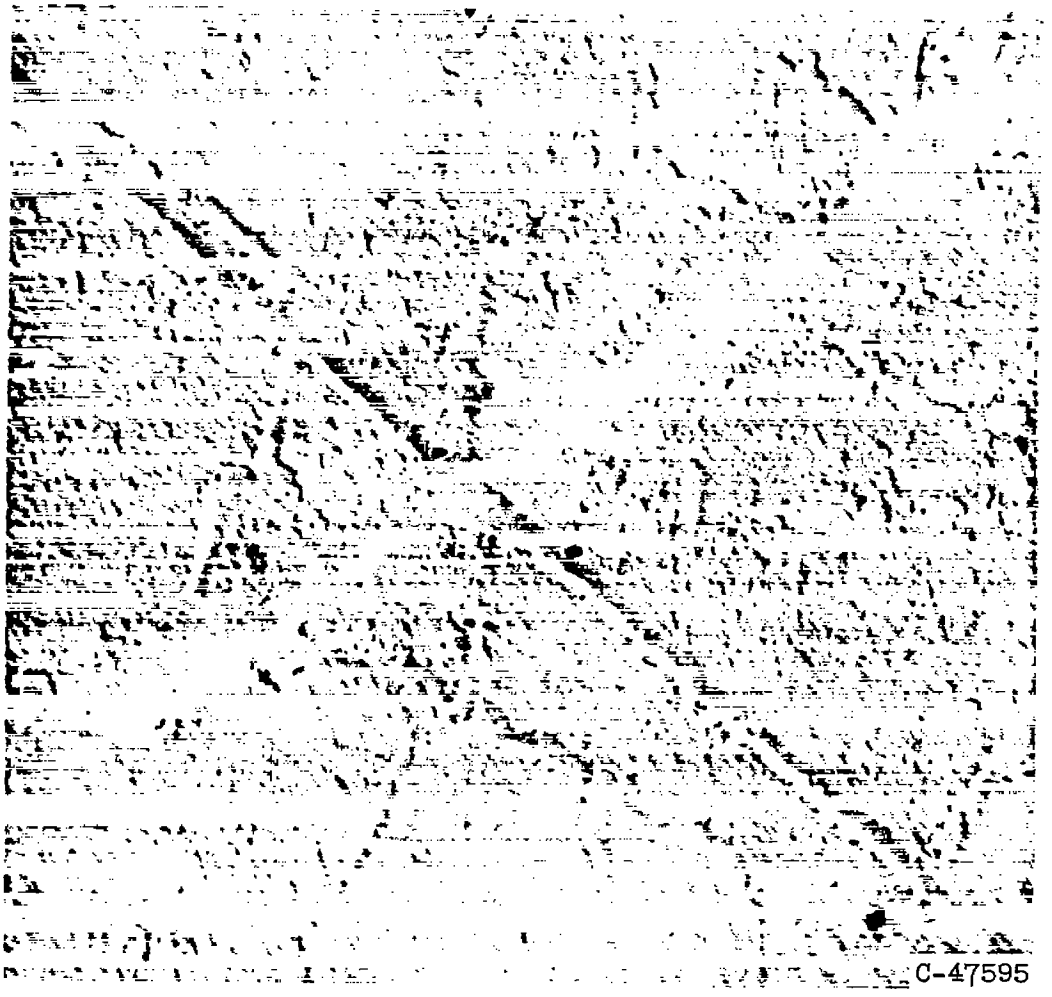

Figure 4. - Electron micrograph of surface of uncharged, large-grain-size Ferrovac E. Platinum preshadowed positive silica replica; X10,000.

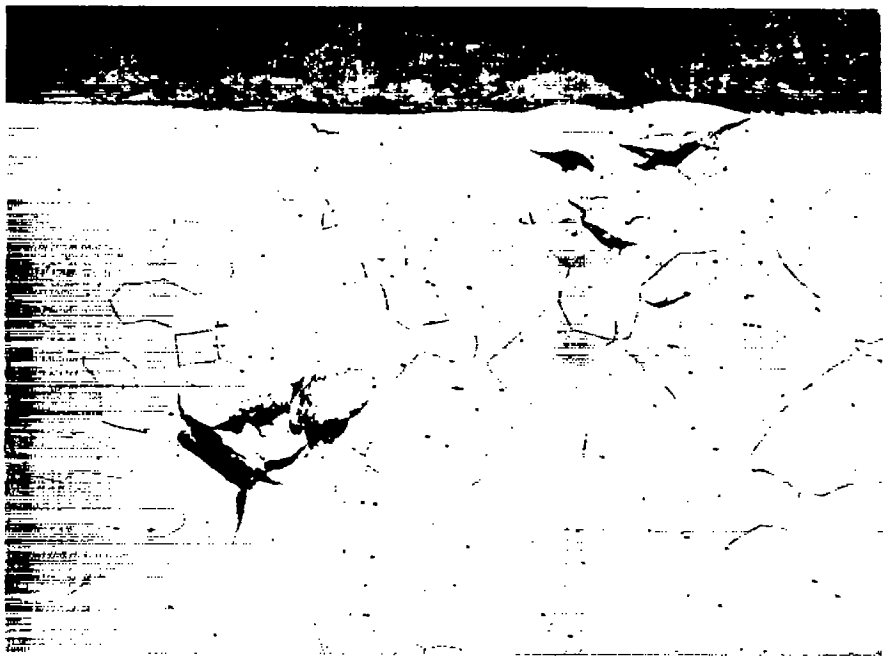

Figure 5. - Large-grain-size Ferrovac E, charged 3 hours. Nital etch; X100.

Figure 6. - Artificial blister on large-grain-size Ferrovac E; X250.

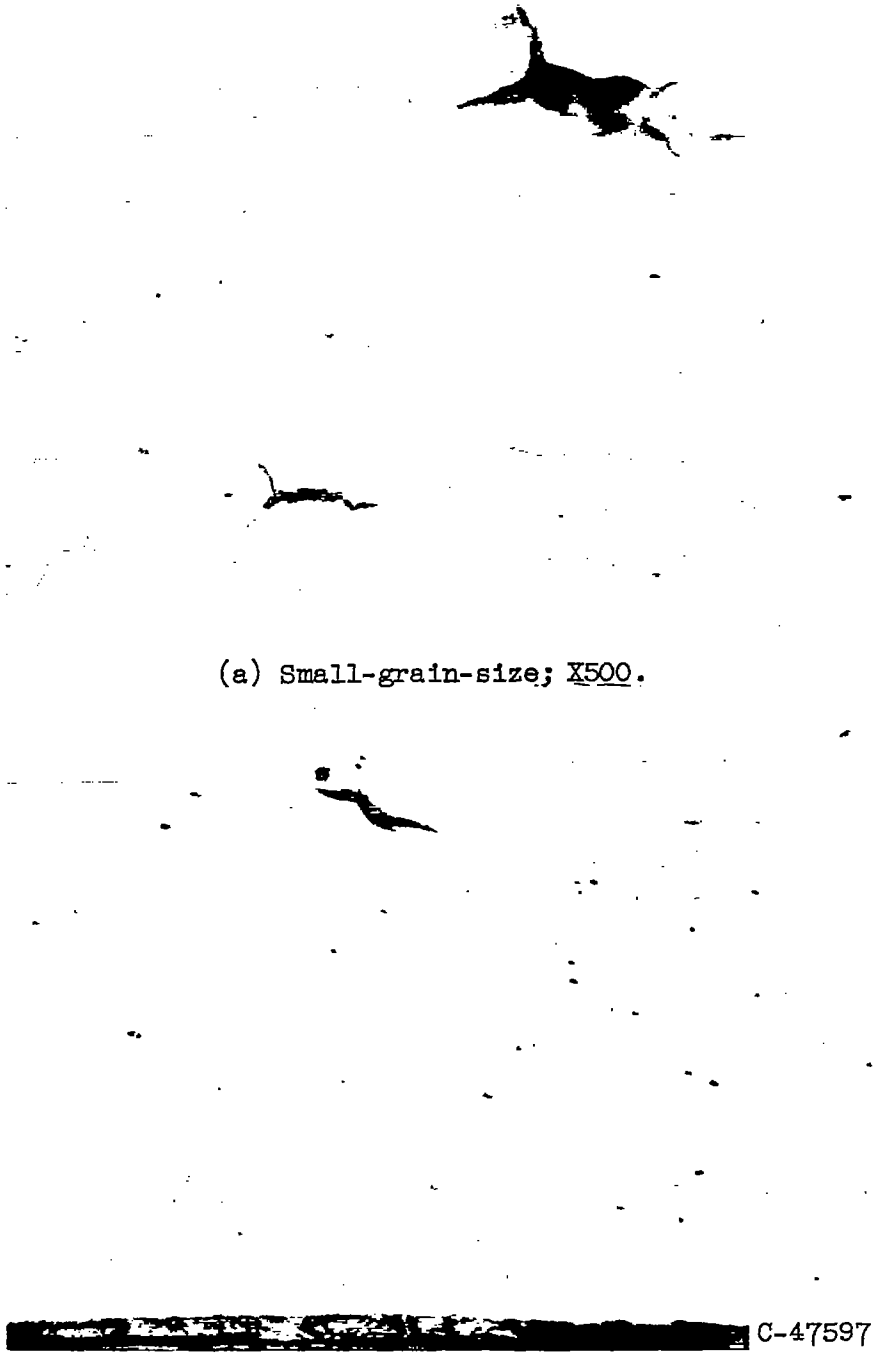

(a) Small-grain-size; X500.

C-47597

(b) Large-grain-size; X250.

Figure 7. - Ferrovac E, charged 10 minutes. Nital etch.

Figure 8. - As-drawn Ferrovac E, charged 18.3 hours. Nital etch; X100.

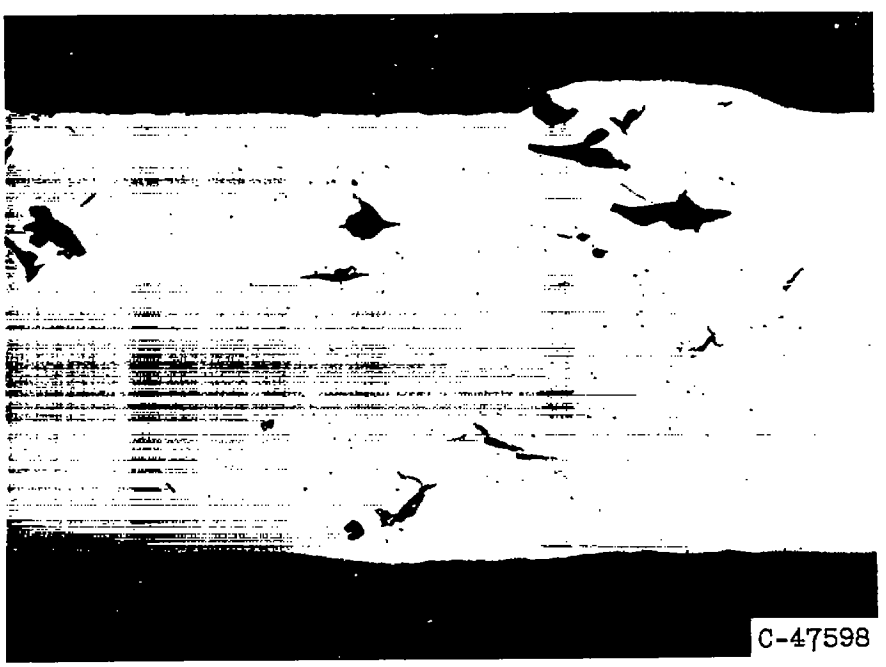

Figure 9. - Single crystal of Ferrovac E, charged 3.5 hours; X50.

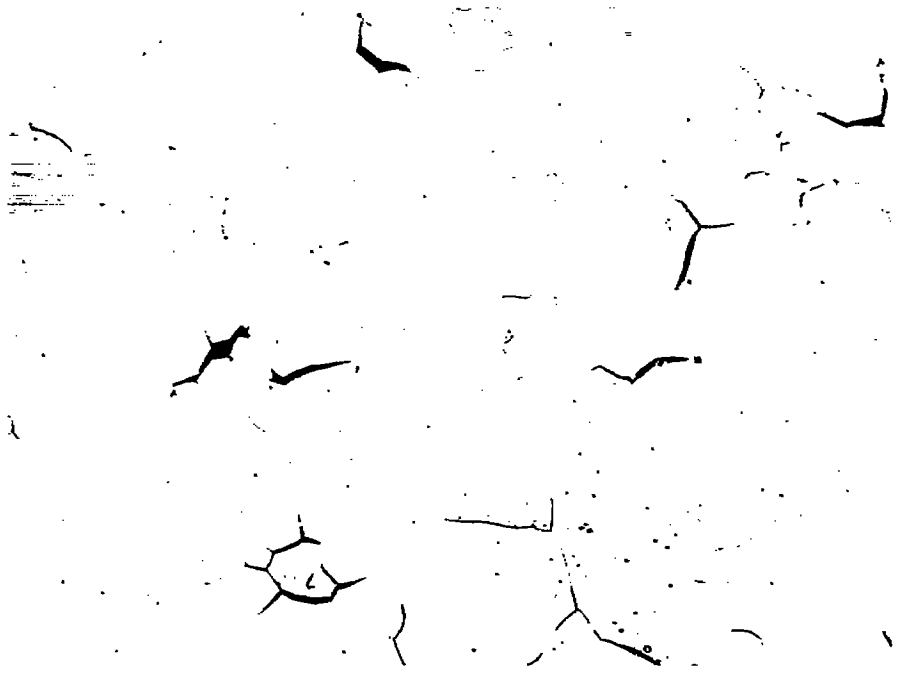

Figure 10. - Large-grain-size Ferrovac E, annealed 24 hours in wet hydrogen at 710° C, charged 5 hours. Nital etch; X100.

C-47599

Figure 11. - Large-grain-size Ferrovac E, annealed 63 hours in dry hydrogen at 710° C, charged $5\frac{1}{2}$ hours. Nital etch; X100.

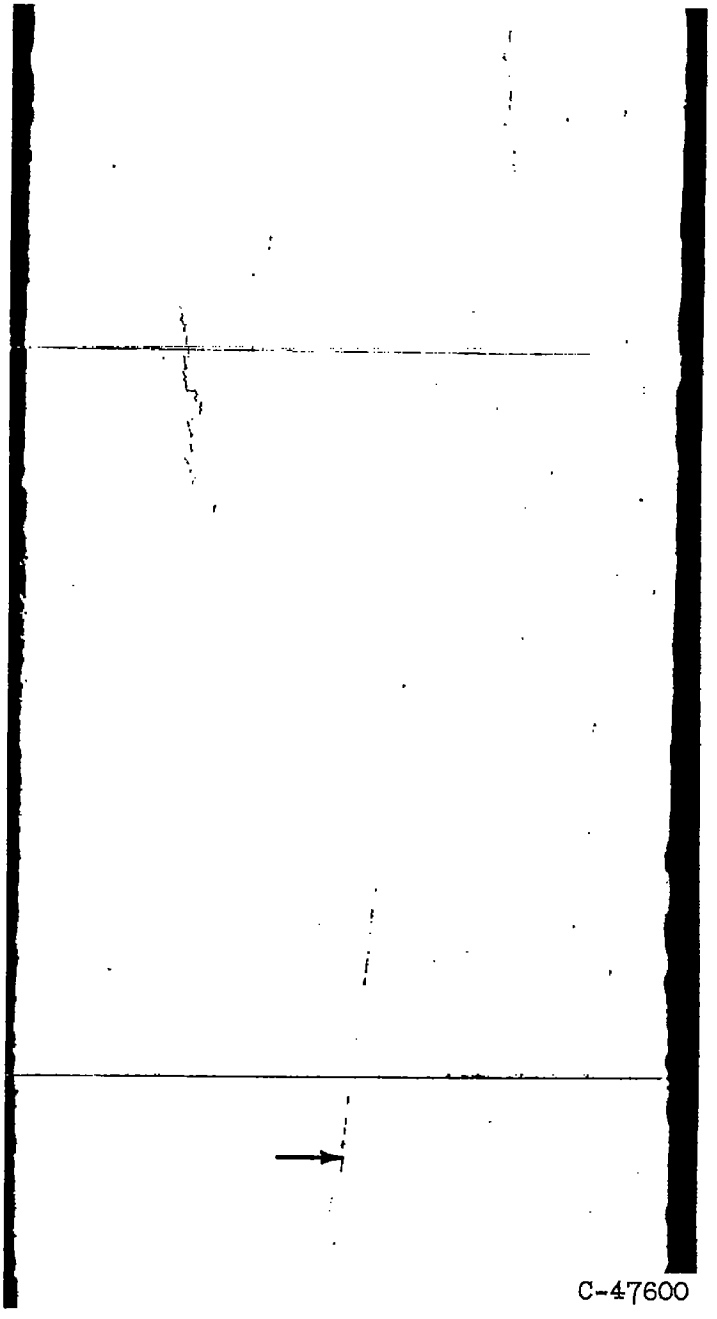

Figure 12. - 370° C tempered 4340 steel, charged 17 hours. As polished; X100.

4932

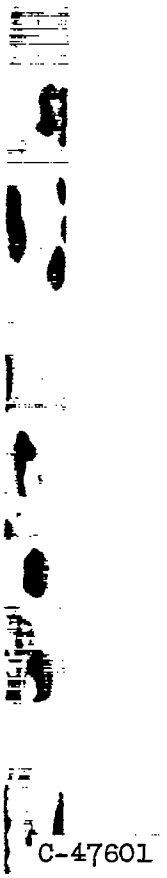

Figure 13. - As-drawn 4340 steel, charged 65 hours; X5.

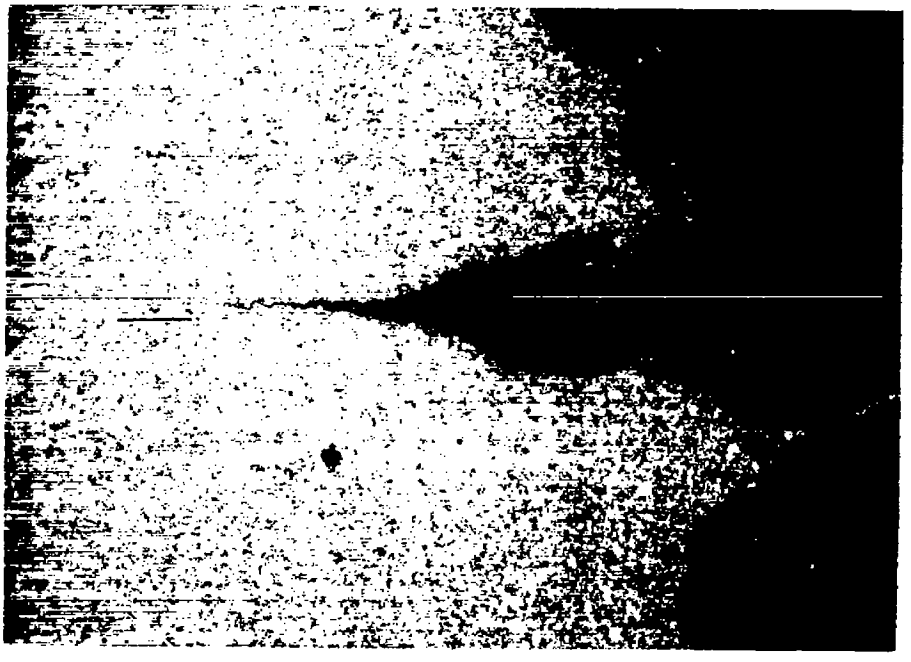

(a) Section normal to specimen axis; X50.

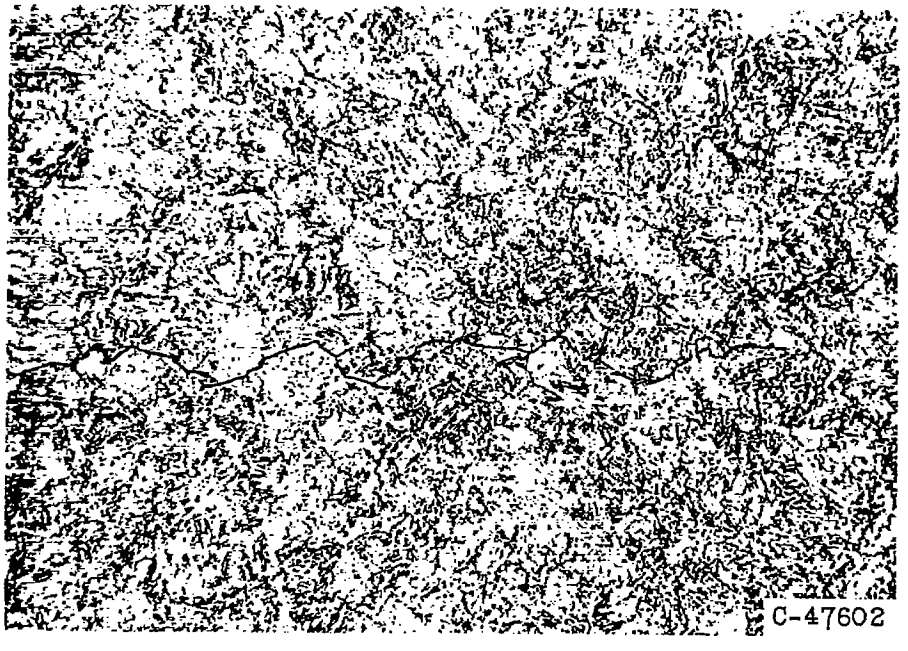

(b) Enlargement of underlined area of 14(a); X500.

Figure 14. - Tempered 4340 steel, charged 24 hours. Picral etch.

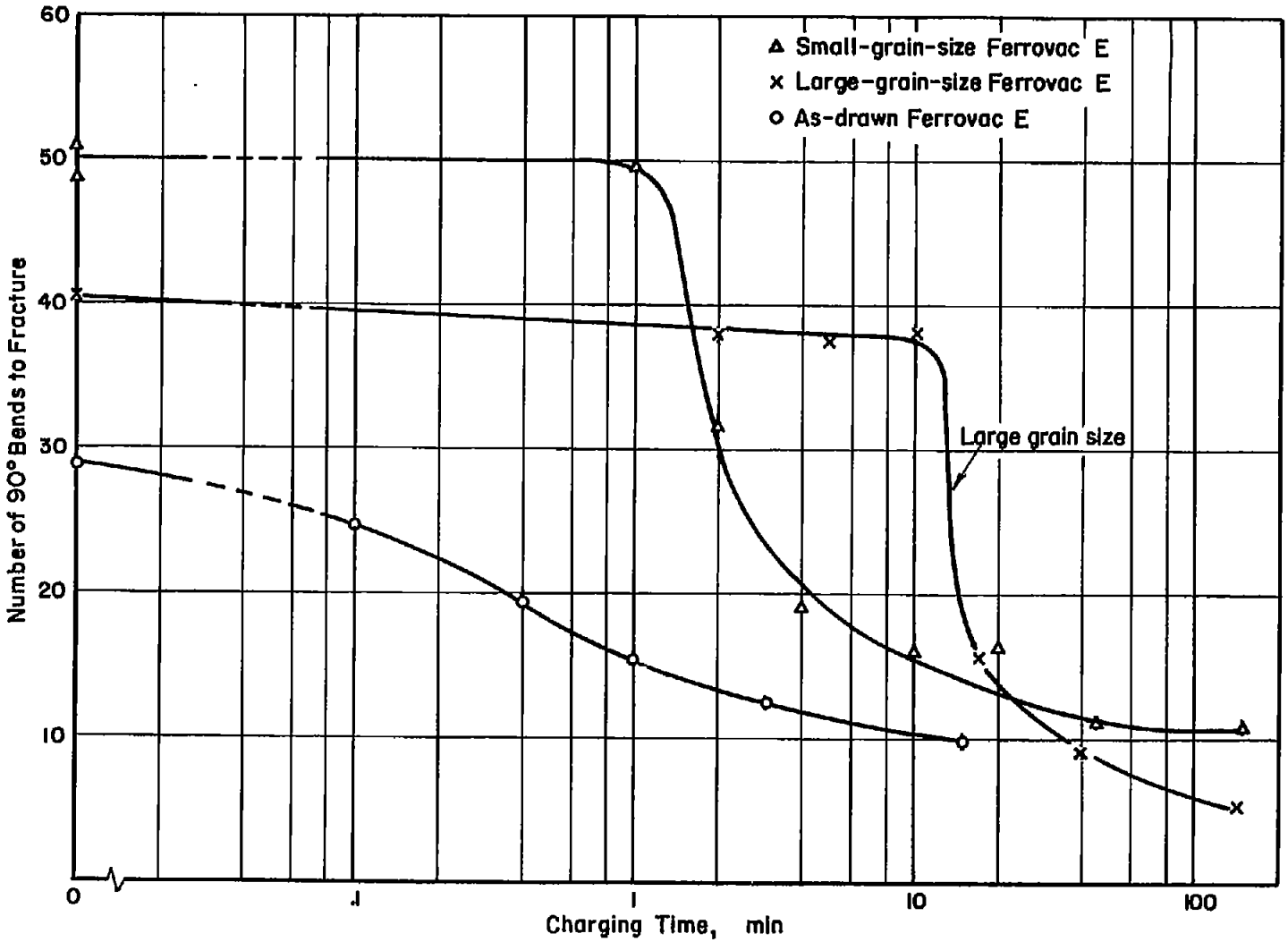

Figure 15. - Effect of cathodic charging on reverse bending for Ferrovac E.

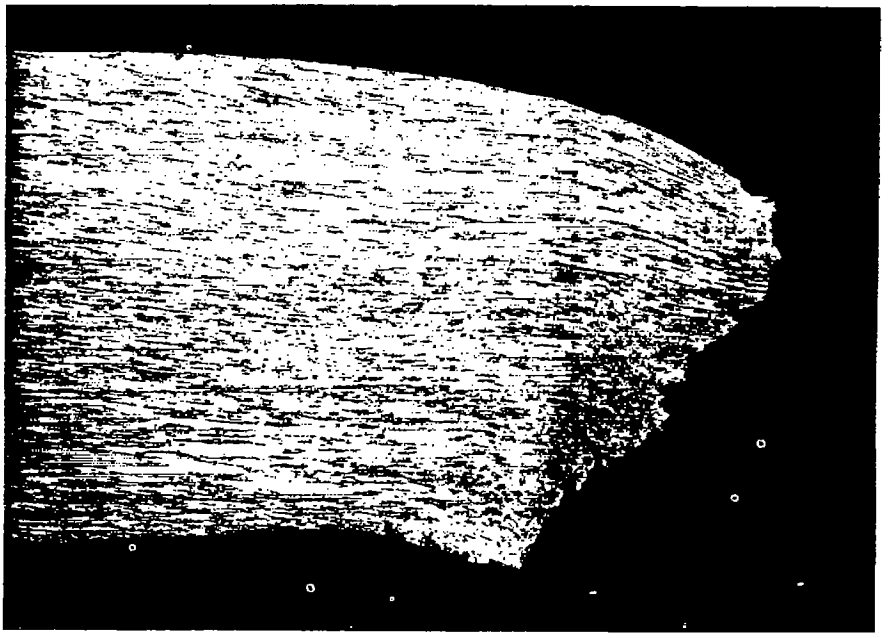

(a) Uncharged. Broke after 29 bends.

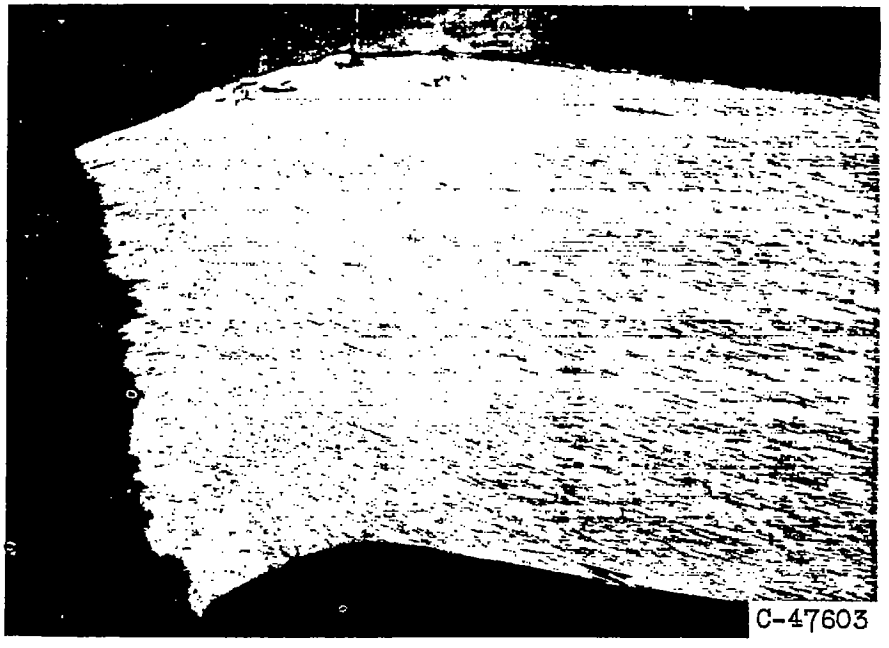

(b) Charged 3 minutes. Broke after $12\frac{1}{2}$ bends.

Figure 16. - As-drawn Ferrovac E, bend tested after various charging times; X50.

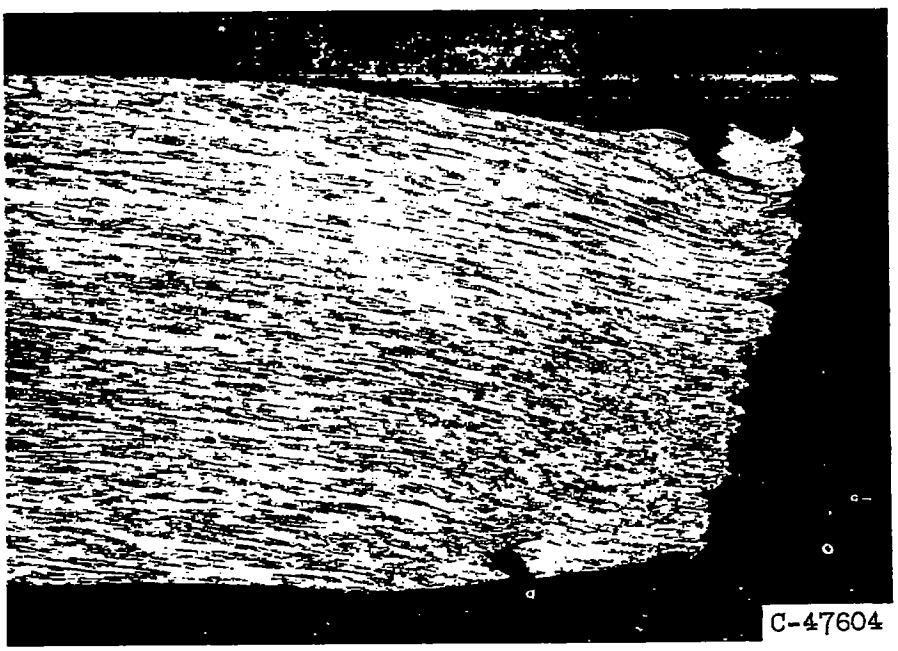

(c) Charged 20 minutes. Broke after 10 bends.

Figure 16. - Concluded.

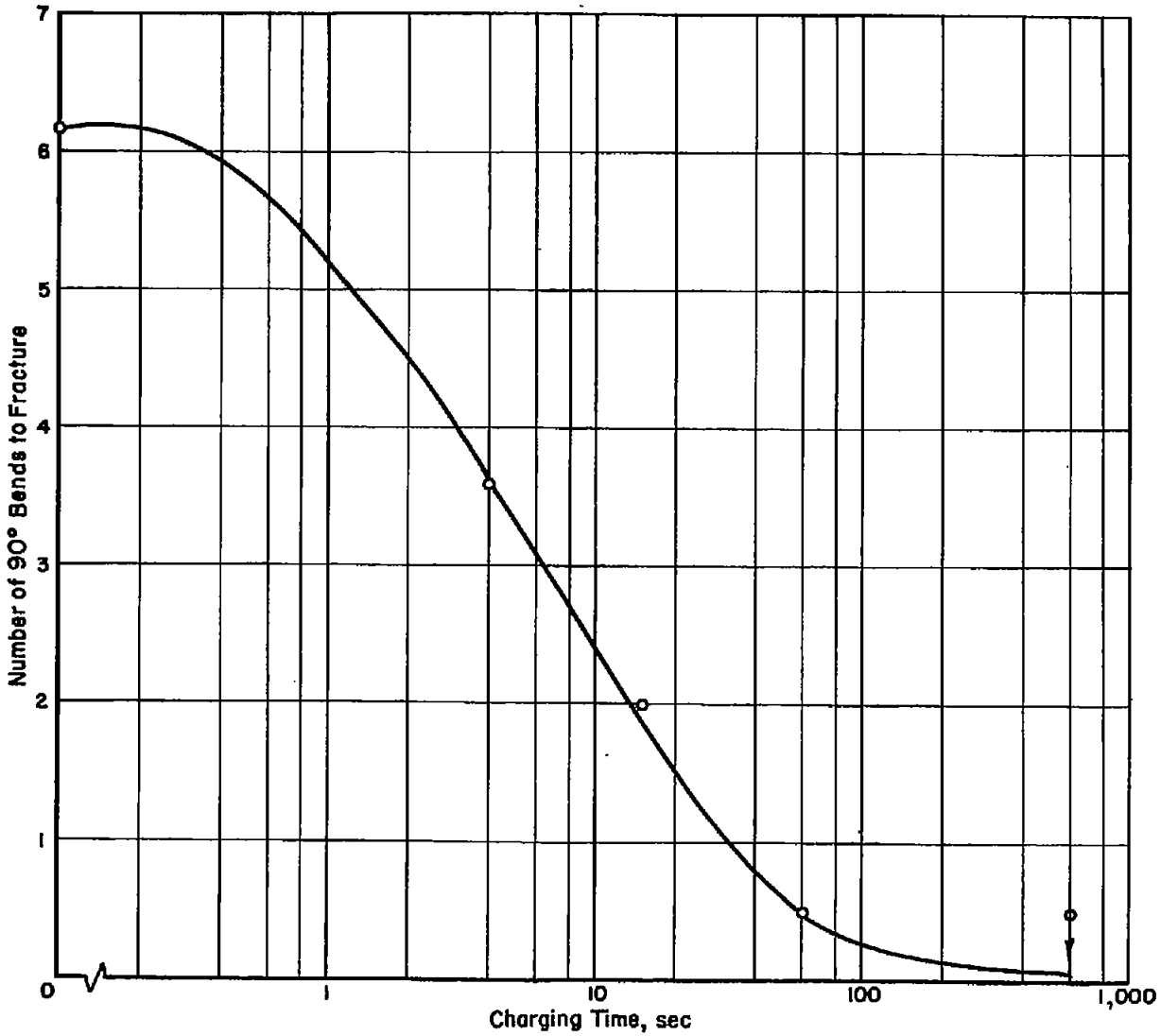

Figure 17. - Effect of charging on reverse bending for 370° C tempered 4340 steel.

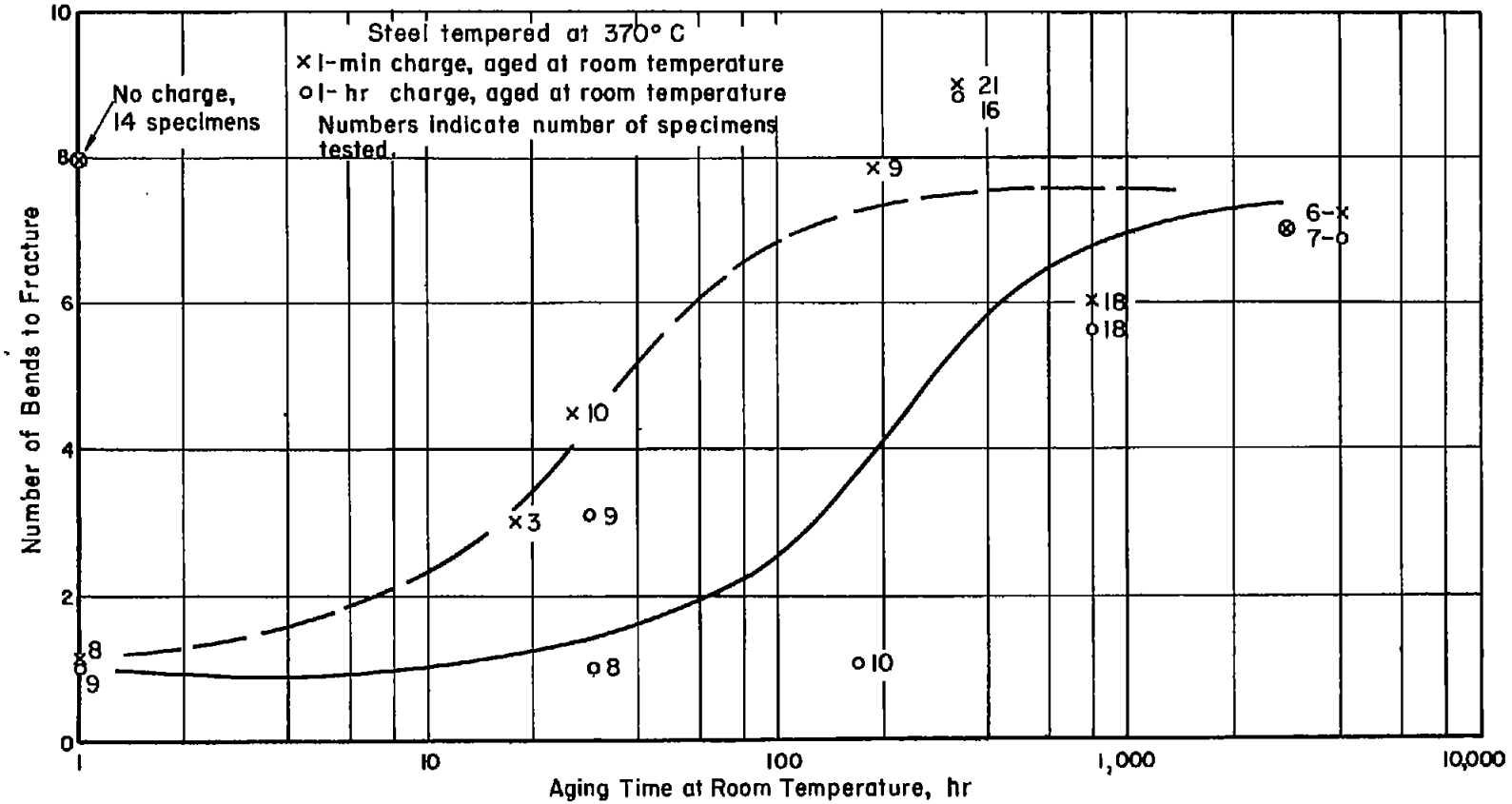

Figure 18. - Effect of room-temperature aging on embrittlement of charged 4340 steel.

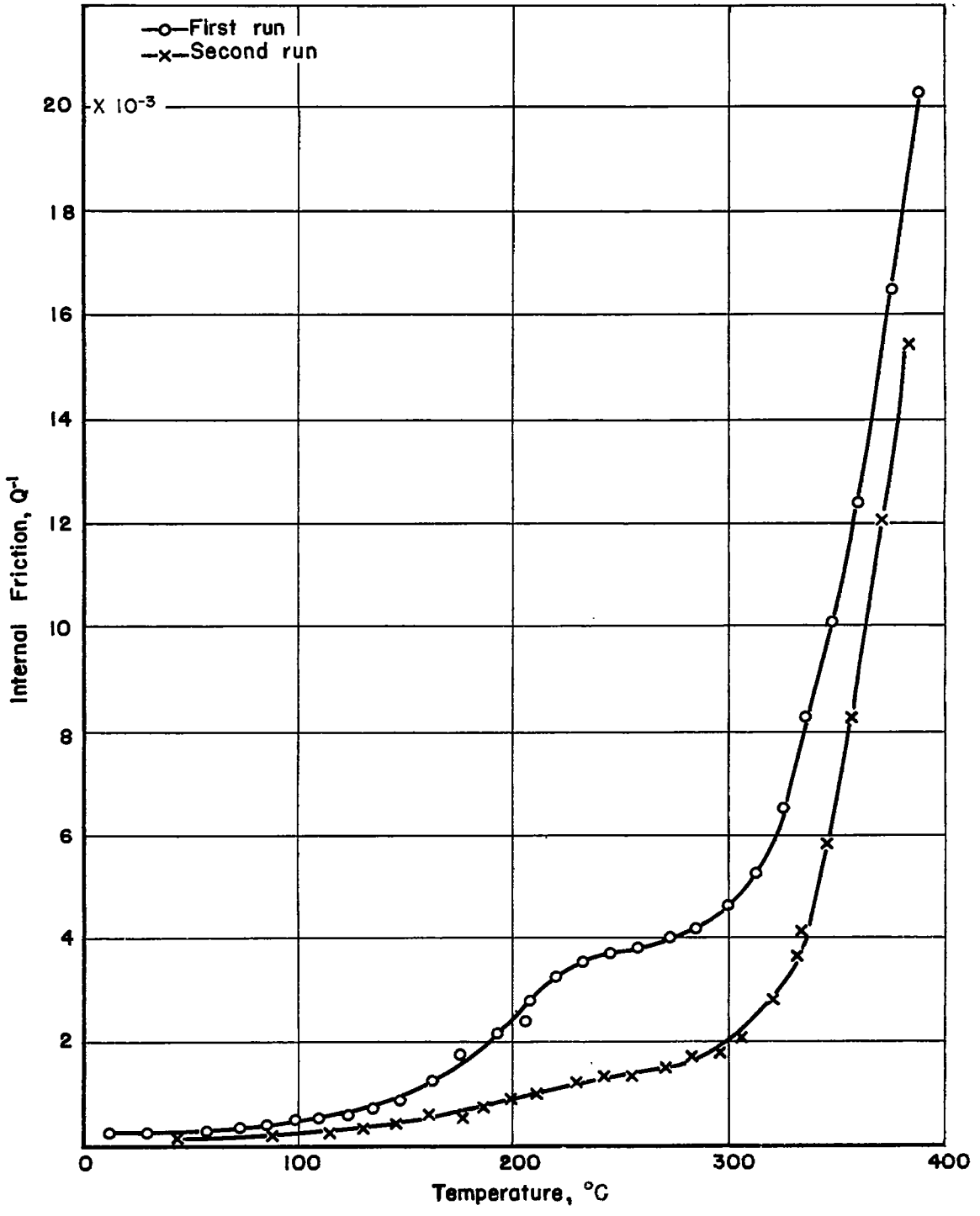

Figure 19. - Variation of internal friction with temperature for as-drawn, uncharged Ferrovac E.

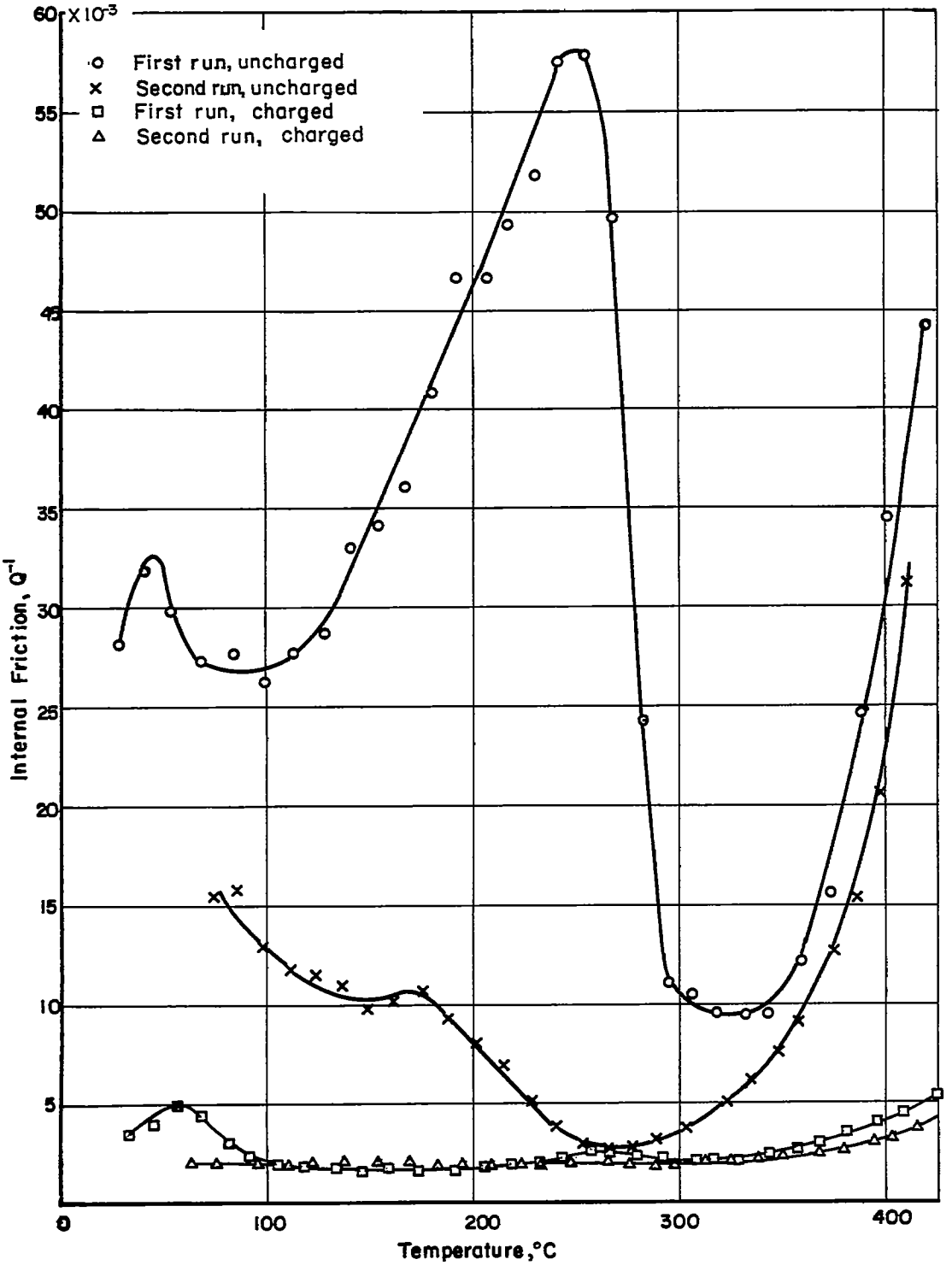

Figure 20. - Variation of internal friction with temperature for very-large-grain-size Ferrovac E.

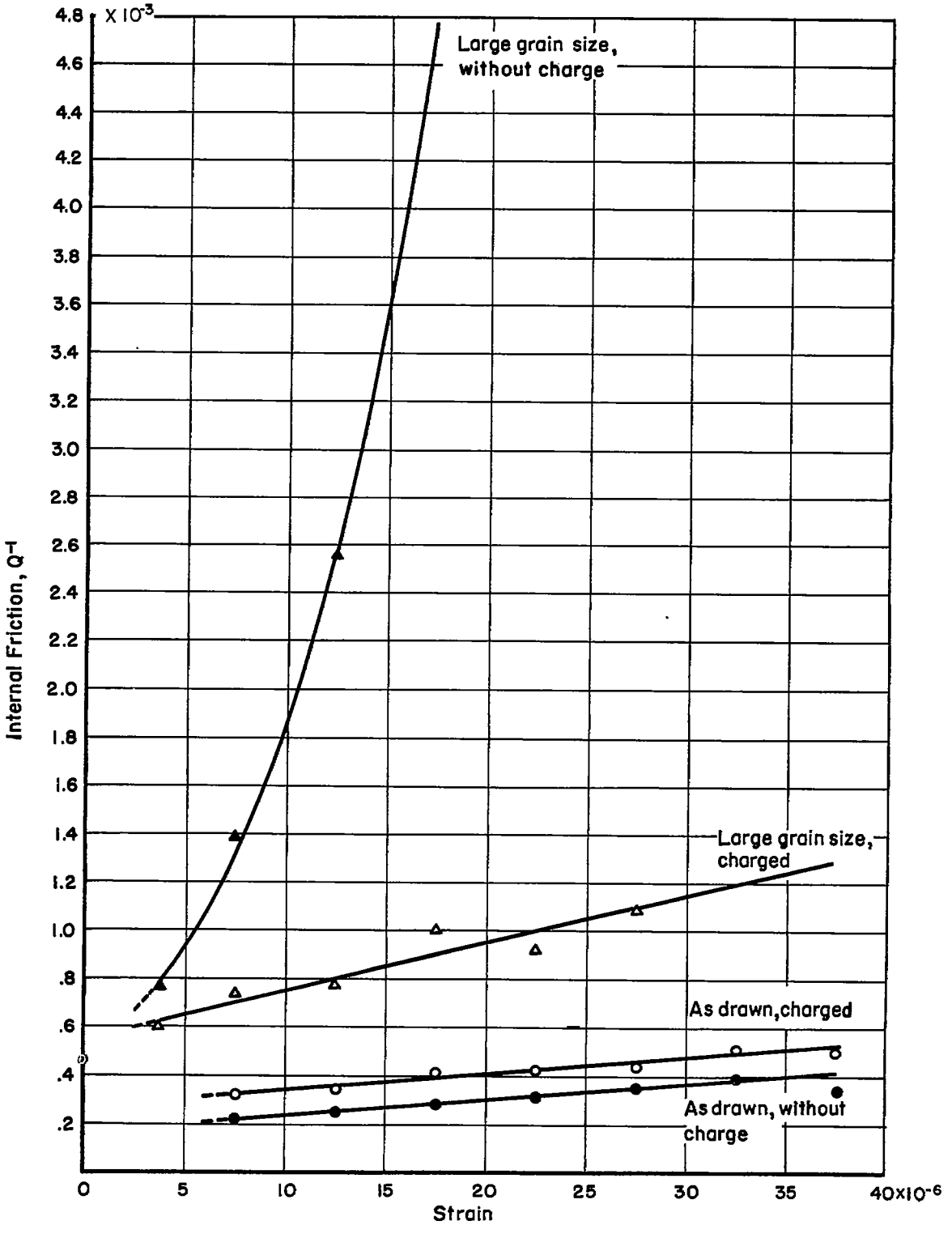

Figure 21. - Dependence of internal friction on strain amplitude for charged and uncharged Ferrovac E at room temperature.

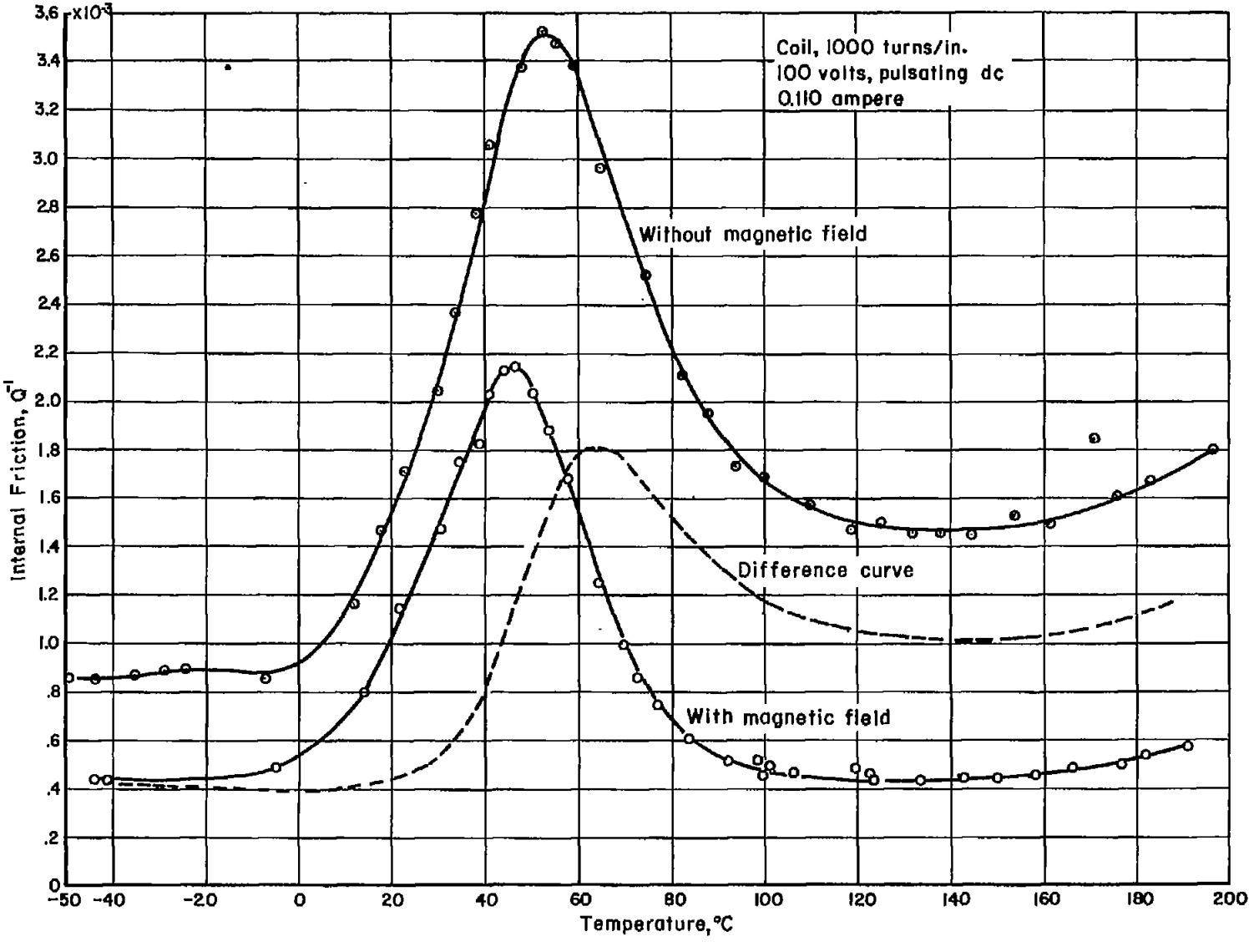

Figure 22. - Damping of Ferrovac E with and without a magnetic field.

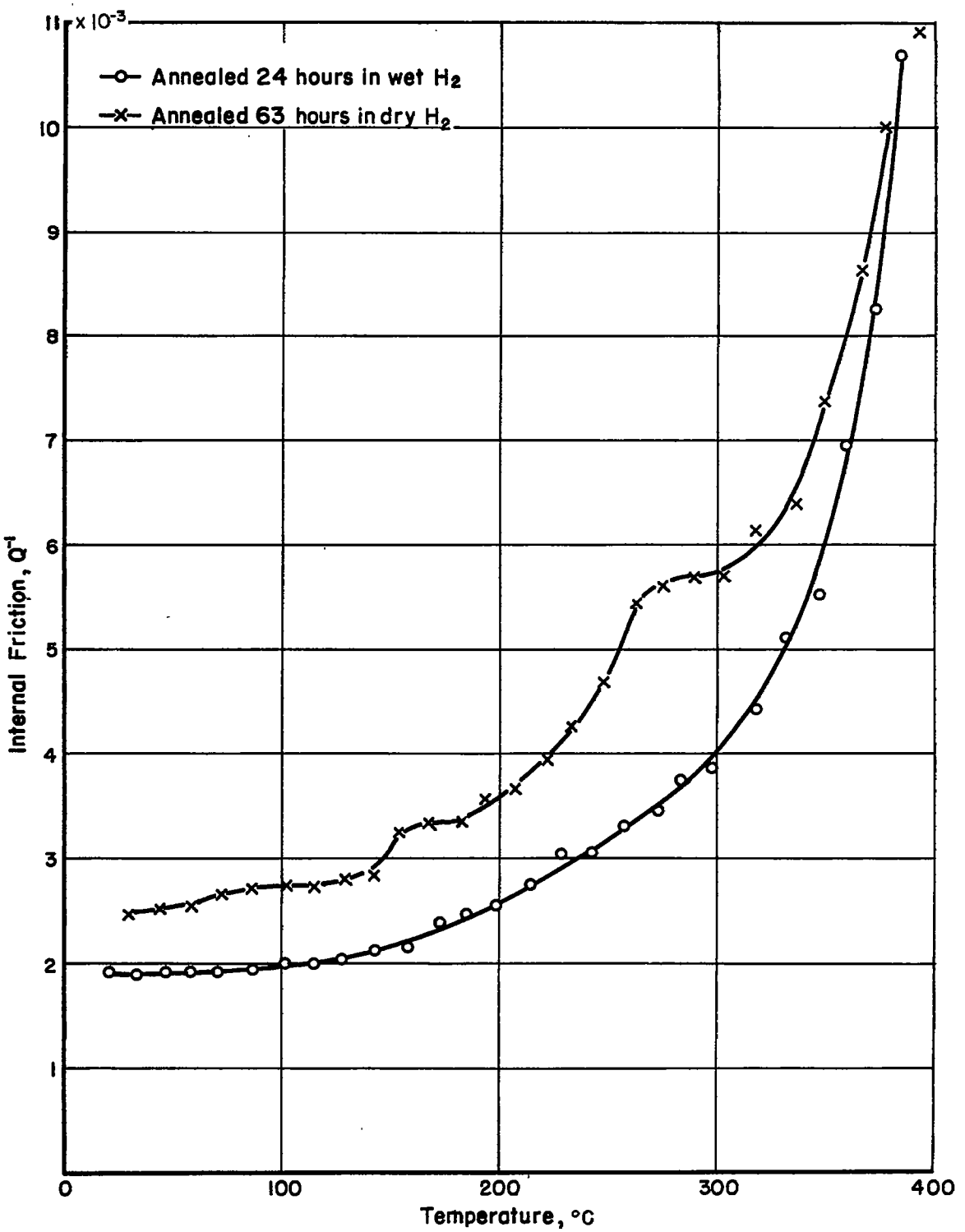

Figure 23. - Variation of internal friction with temperature for hydrogen-annealed large-grain-size Ferrovac E.

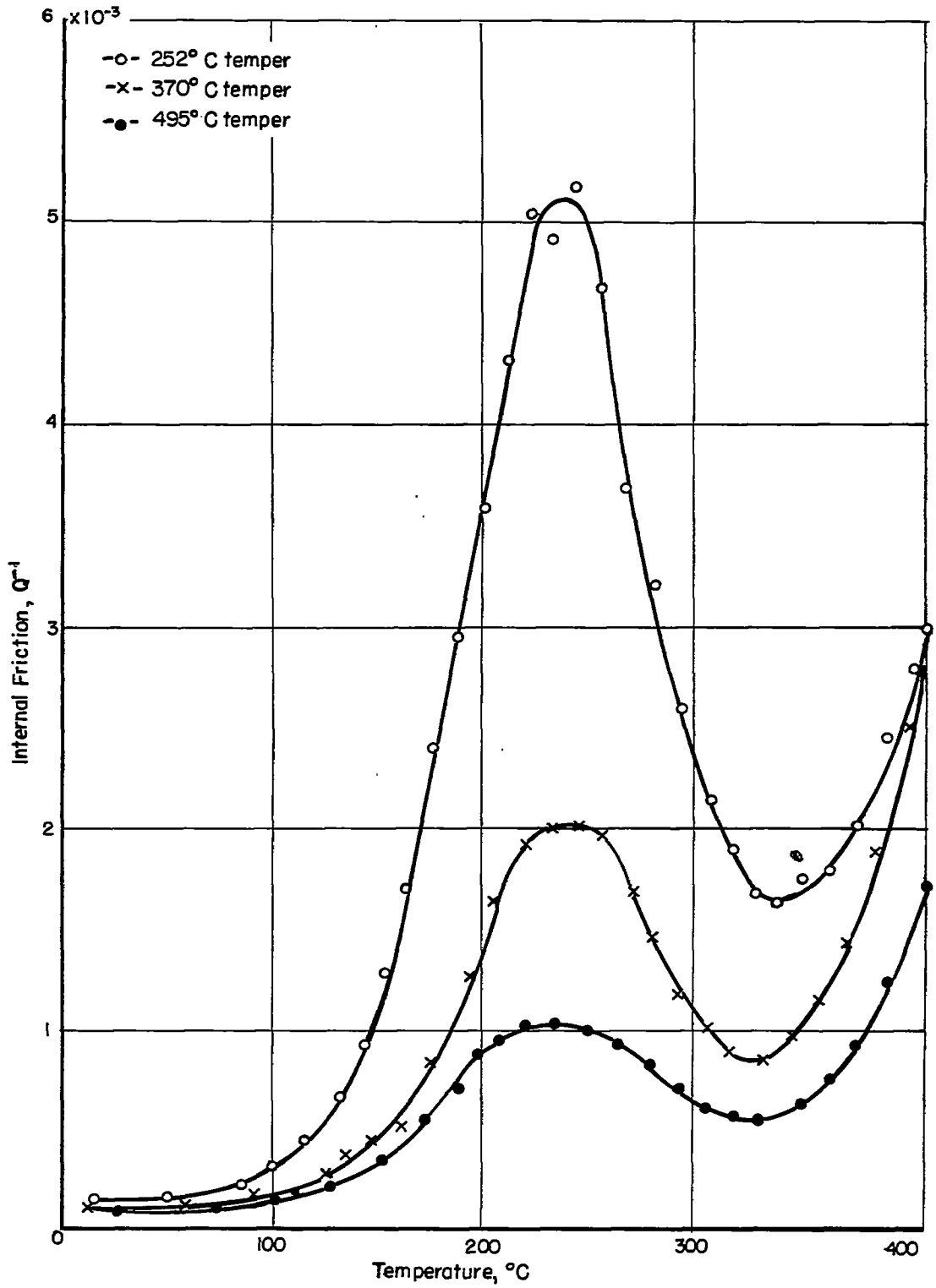

Figure 24. - Variation of internal friction with temperature for 4340 steel after various tempers.

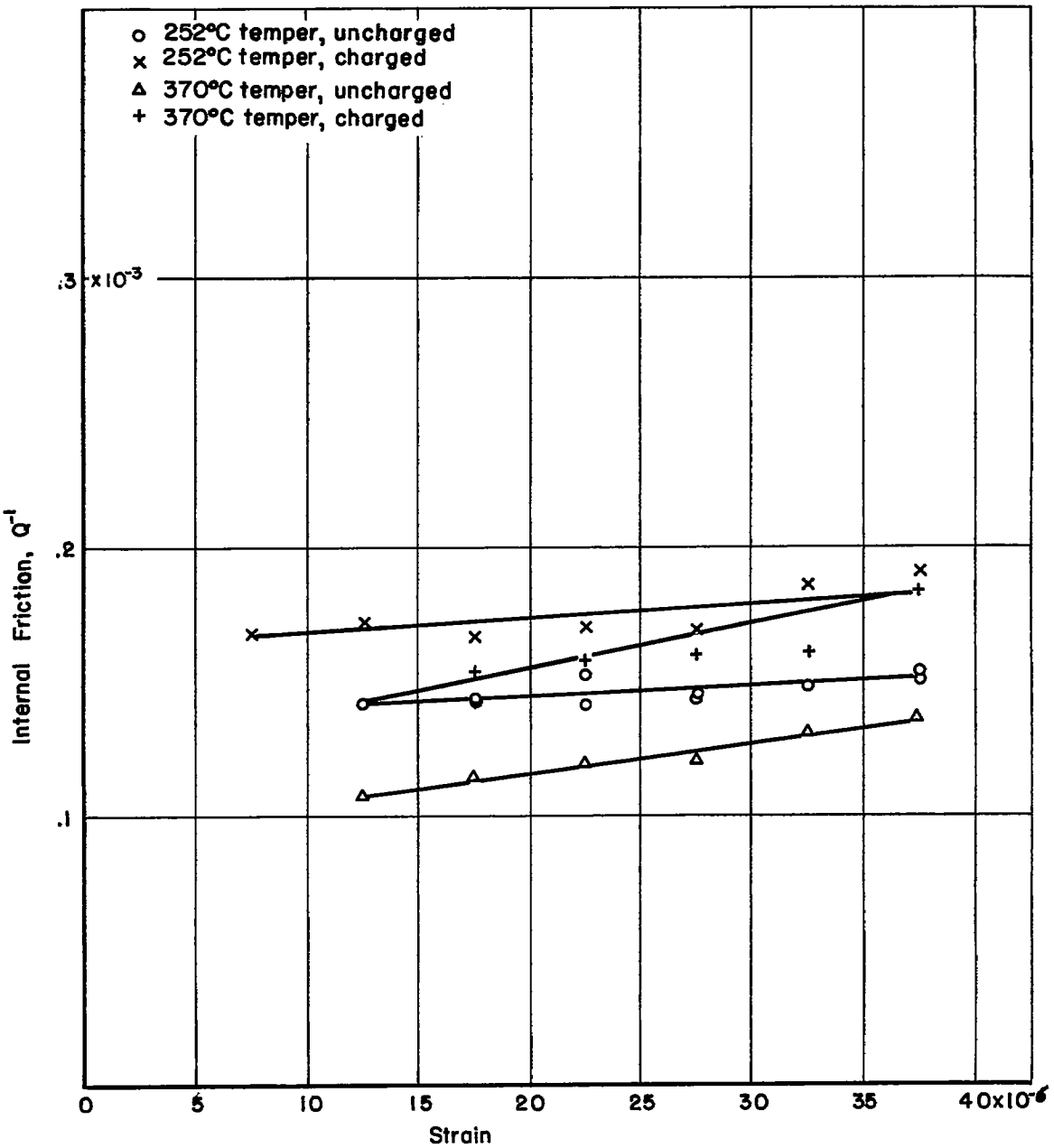

Figure 25. - Effect of charging on amplitude dependence of internal friction of tempered 4340 steel at room temperature.

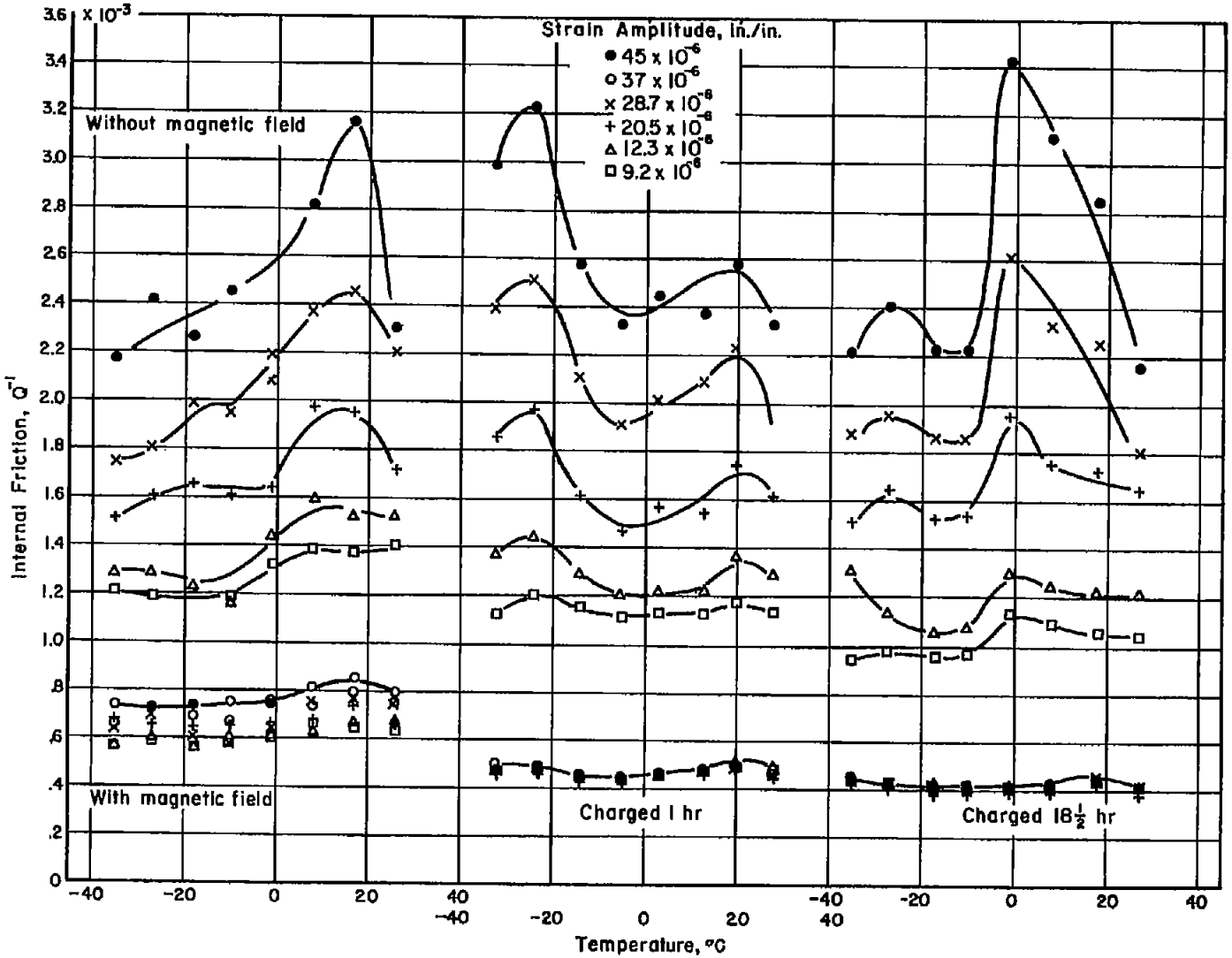

Figure 26. - Effect of glow discharge on damping of Ferrovac E at various strain amplitudes.

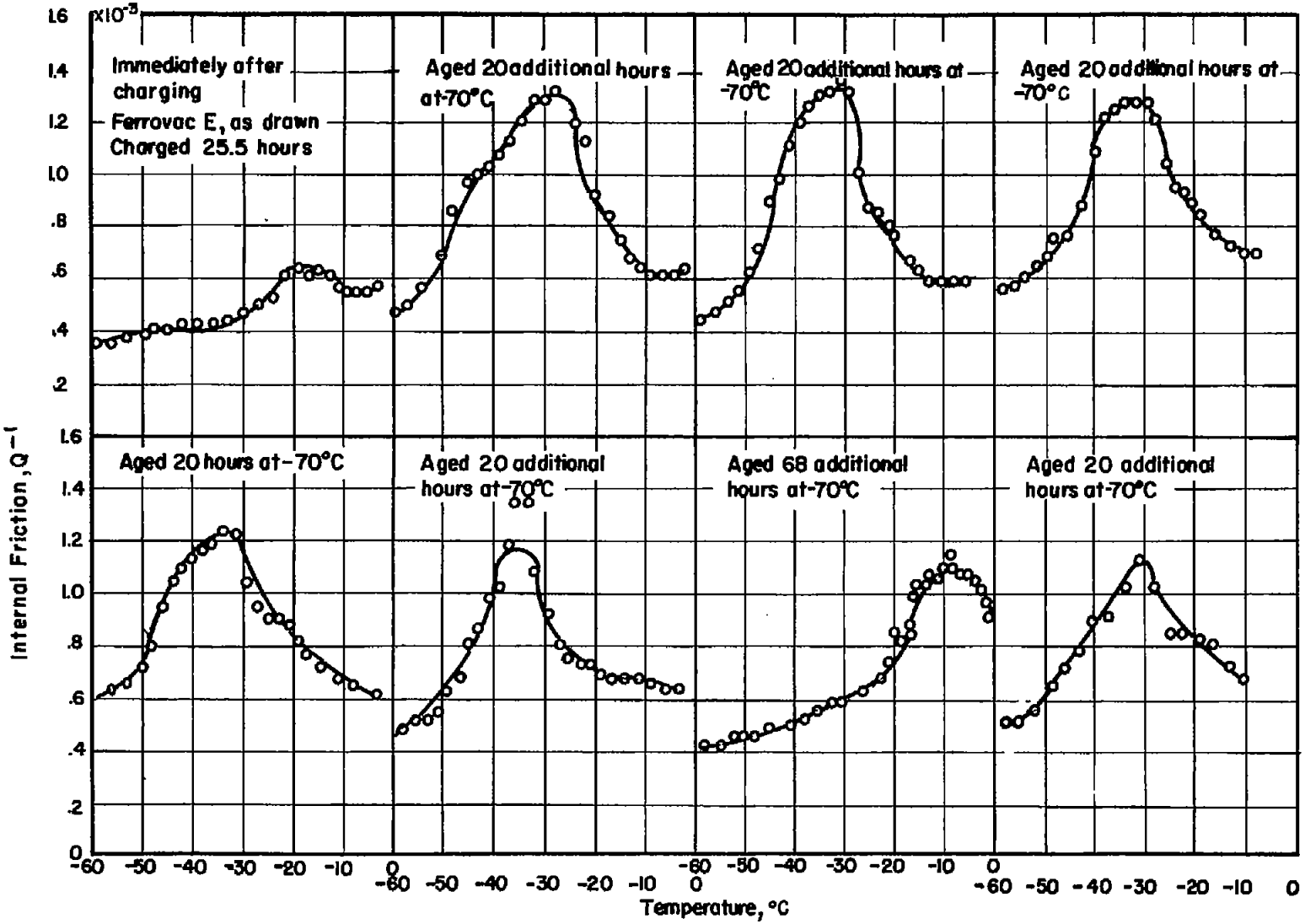

Figure 27. - Sequence of internal-friction - temperature tests showing lack of reproducibility of peak in -10° to -40° C range.

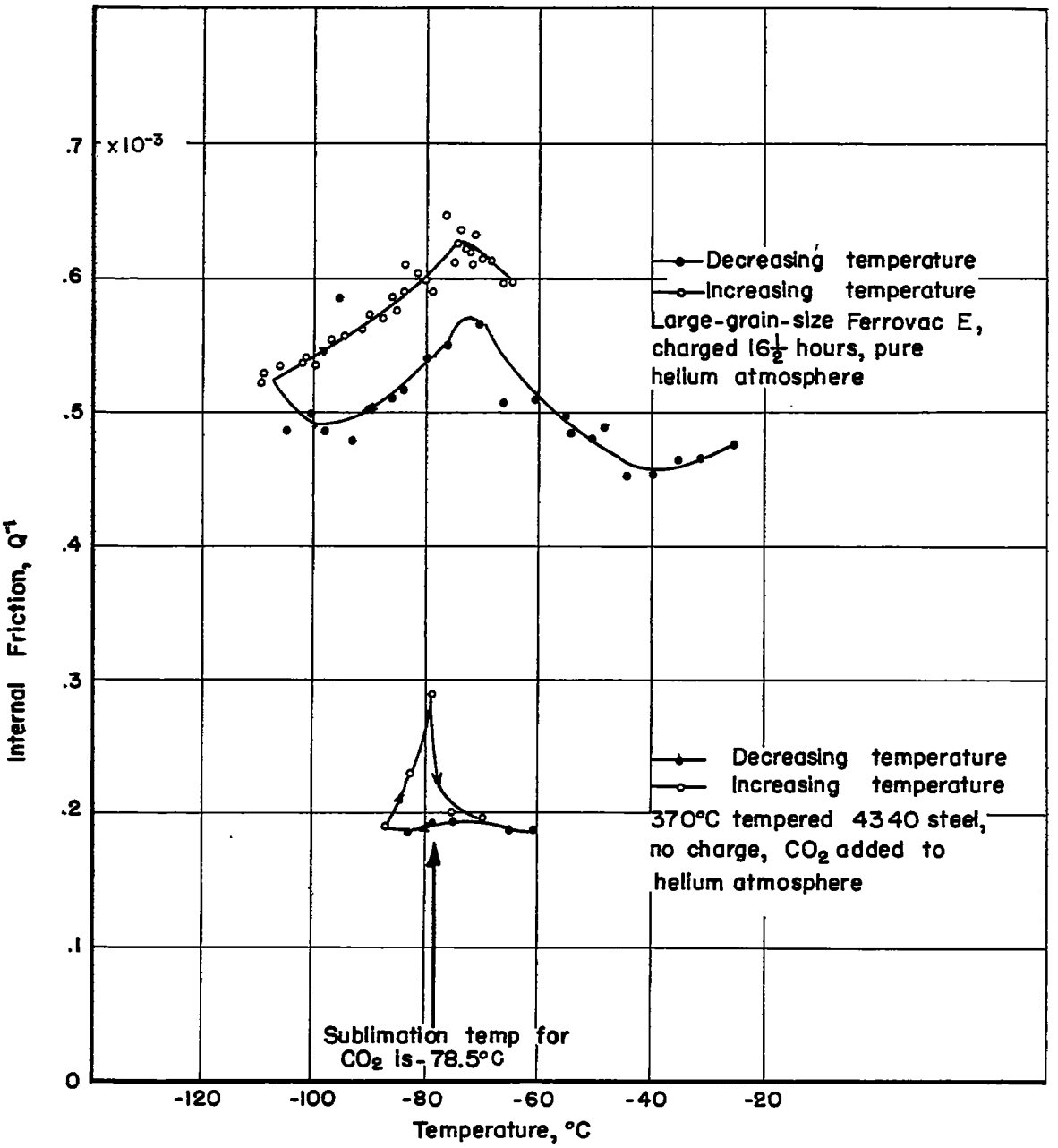

Figure 28. - Comparison of -73° C peak with peak due to presence of CO_2.

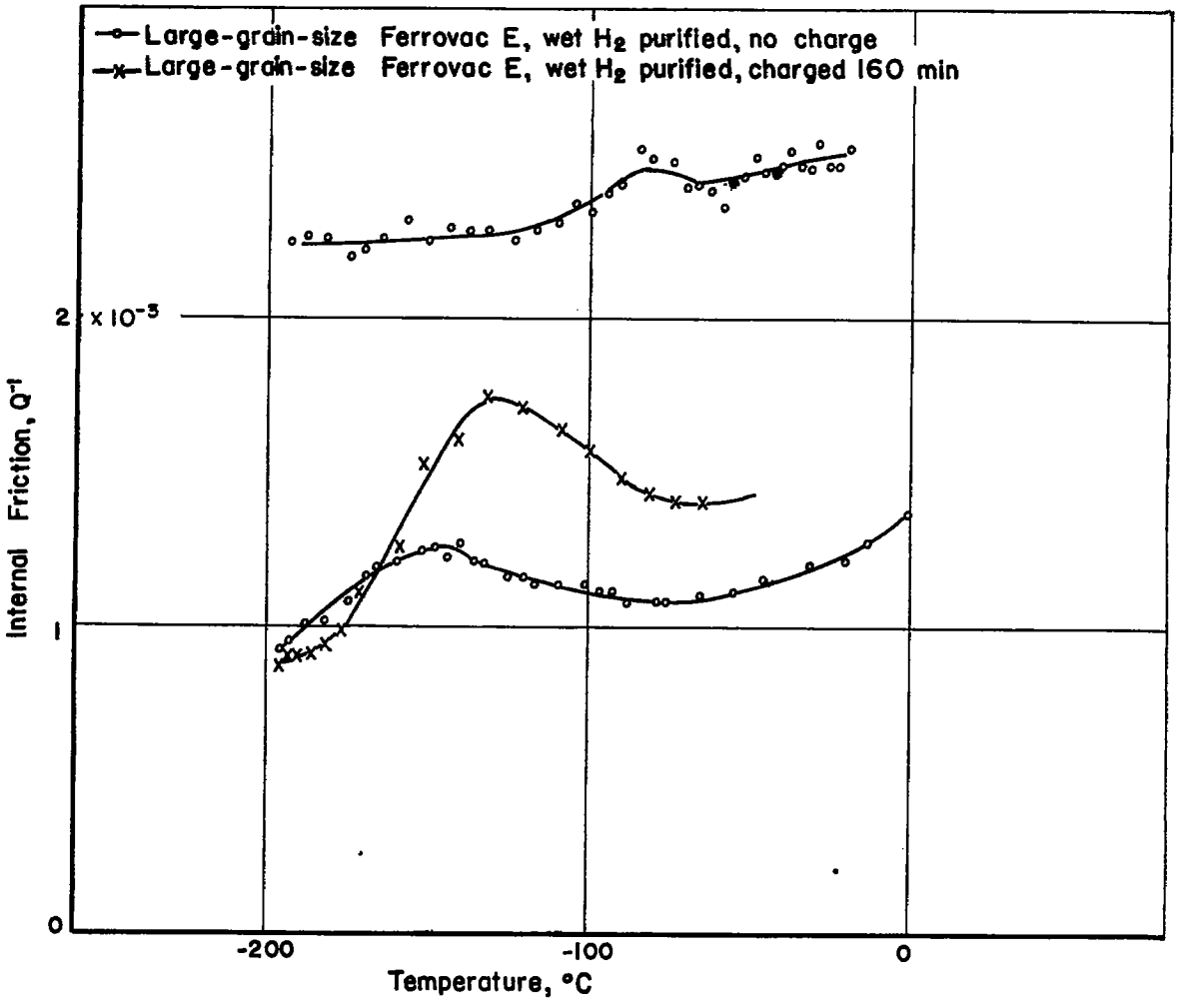

Figure 29. - Variation of internal friction with temperature for wet-hydrogen-purified Ferrovac E.

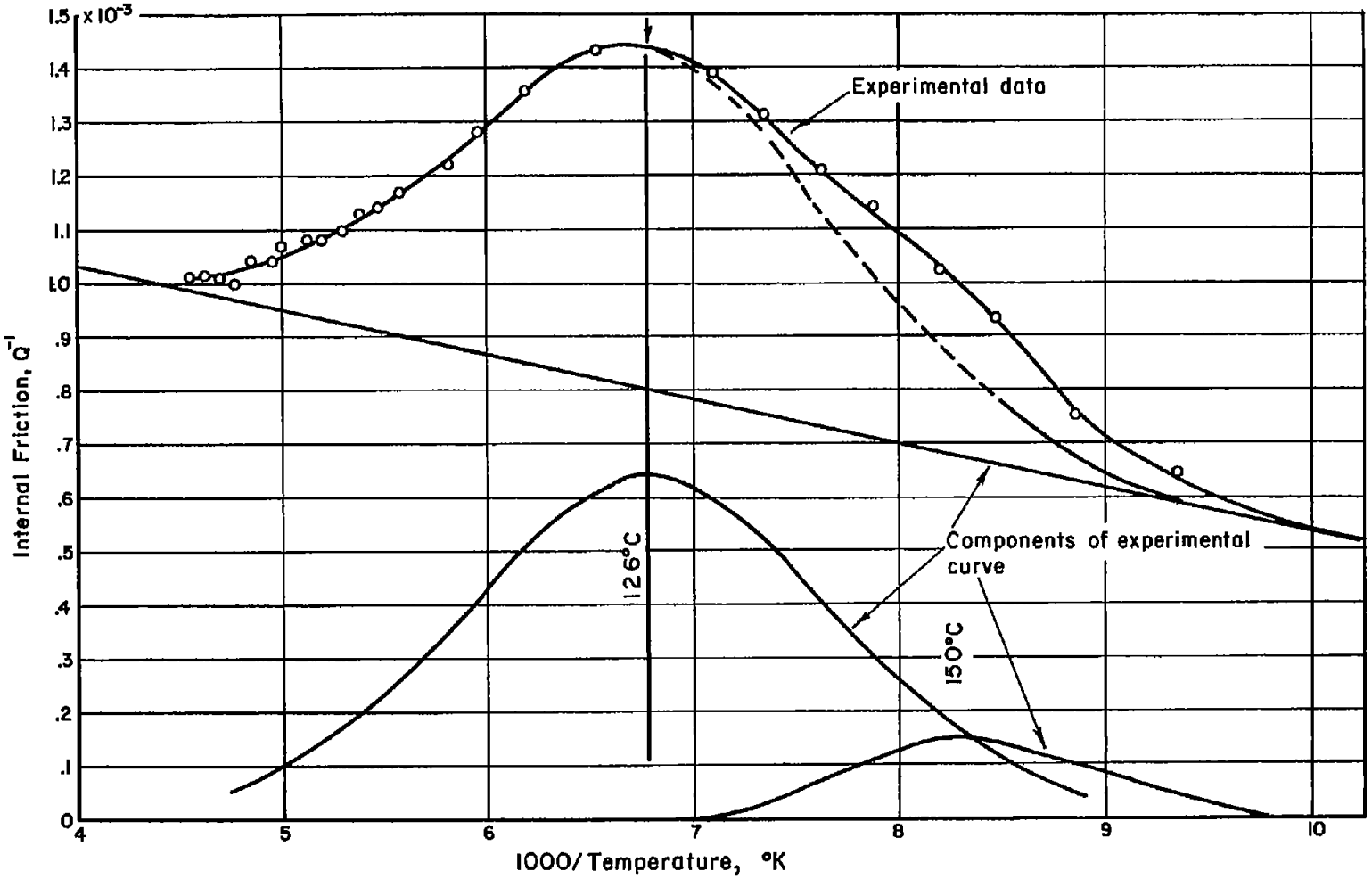

Figure 30. - Hydrogen-induced internal-friction peaks in charged Ferrovac E.

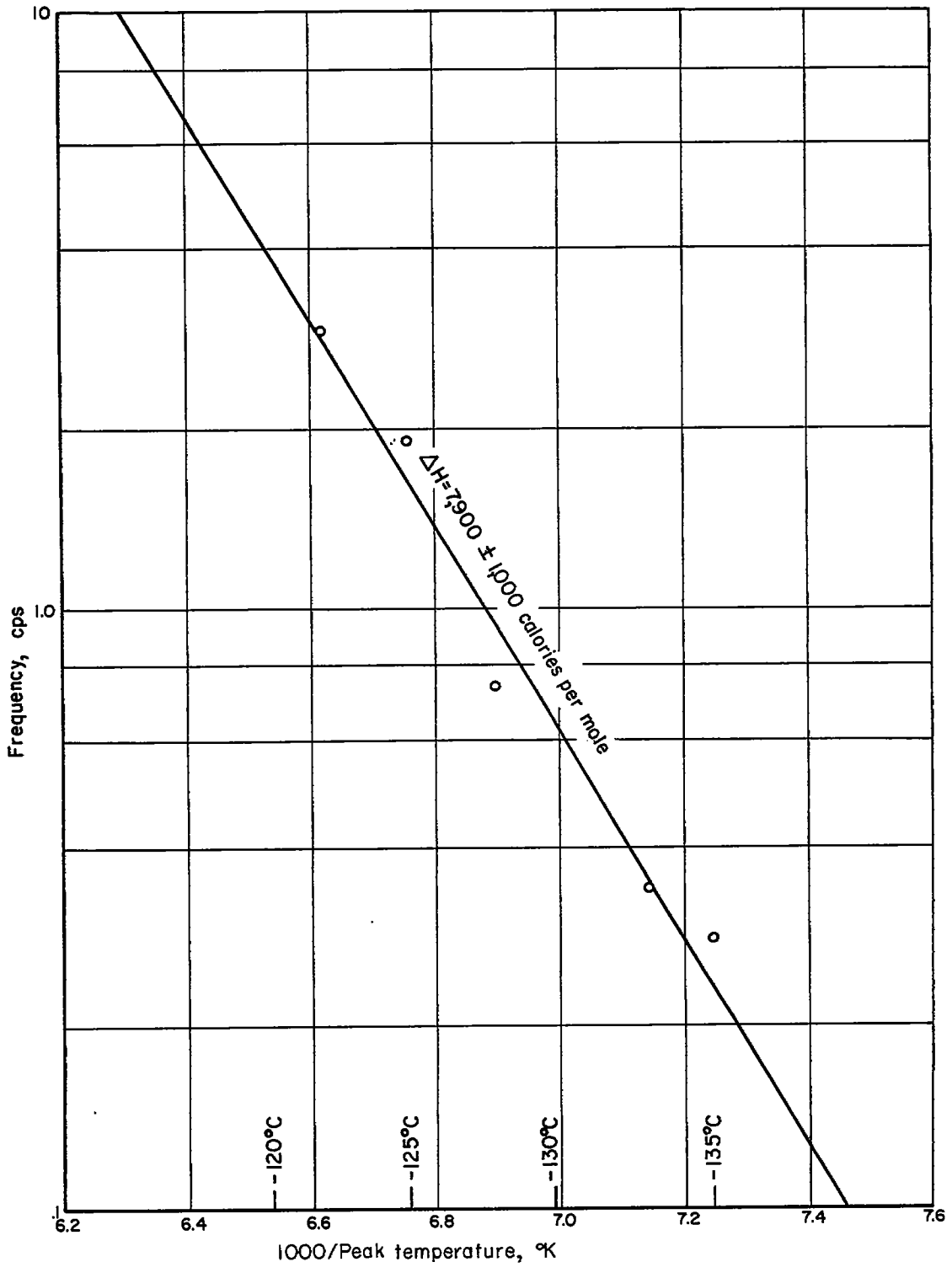

Figure 31. - Frequency dependence of -130° C peak in charged Ferrovac E.

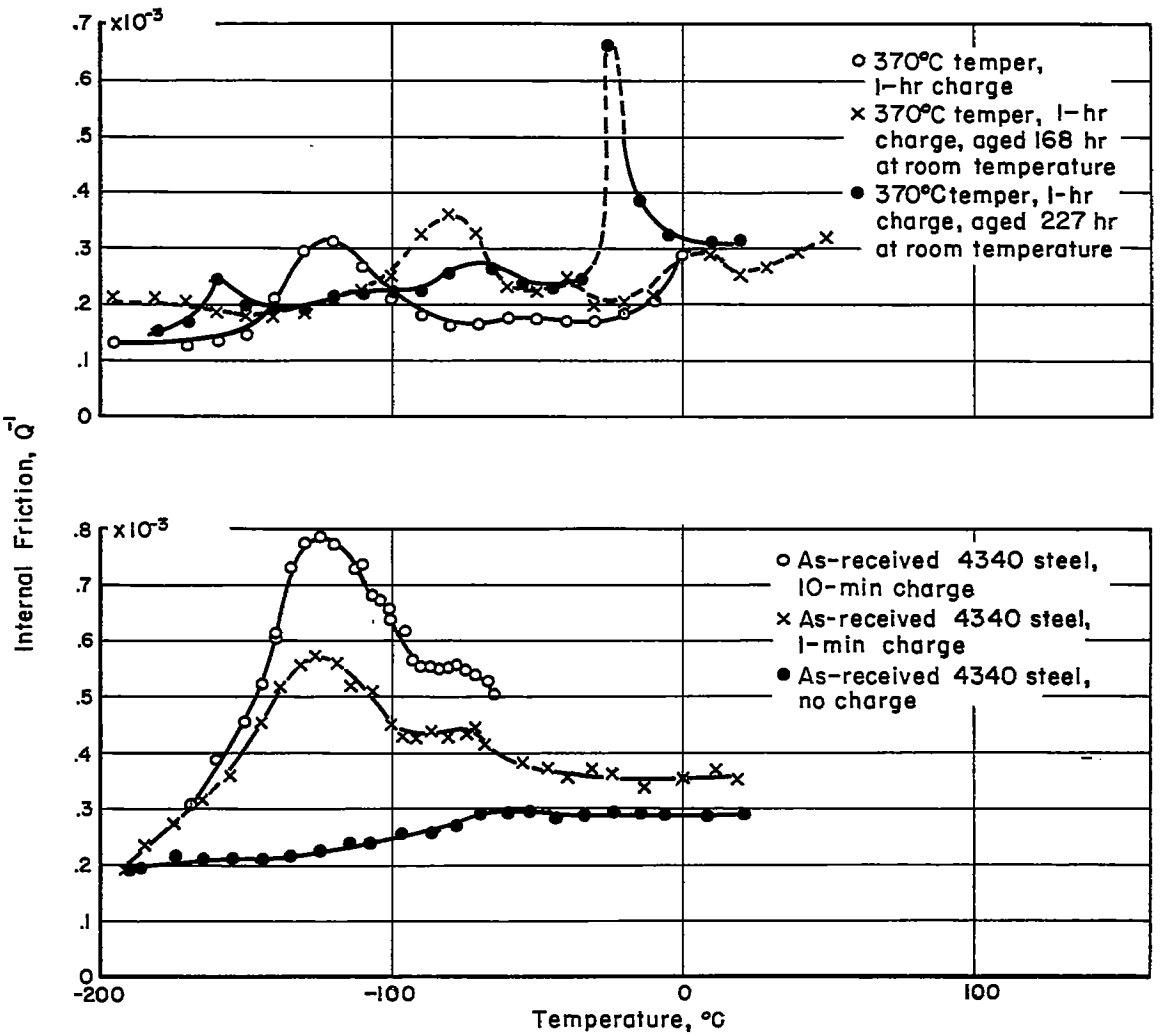

Figure 32. - Hydrogen-induced internal-friction phenomena in charged 4340 steel.

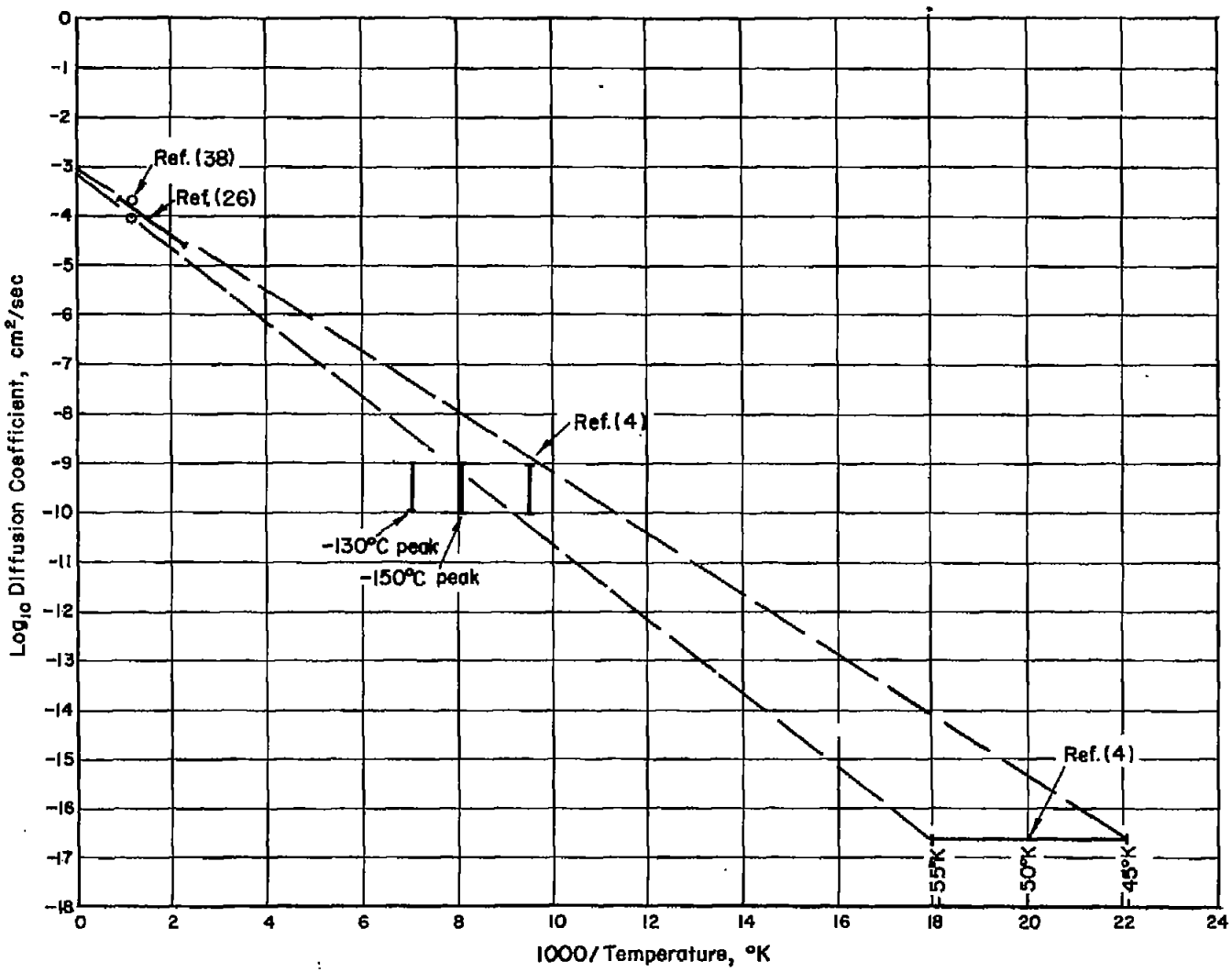

Figure 33. - Variation of diffusion coefficient with temperature for hydrogen in iron.

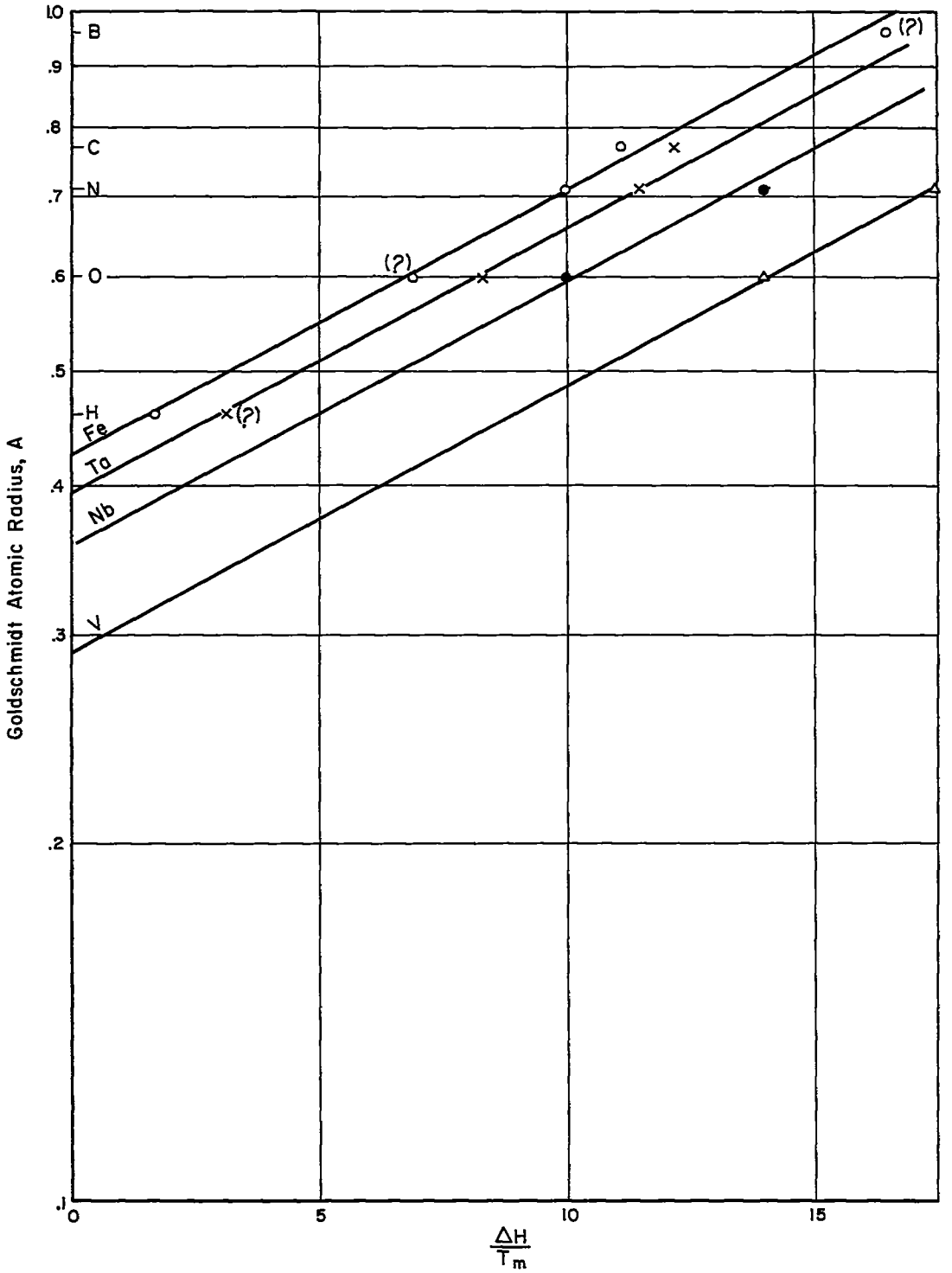

Figure 34. - Empirical correlation of diffusion activation energies and solute atom radii.

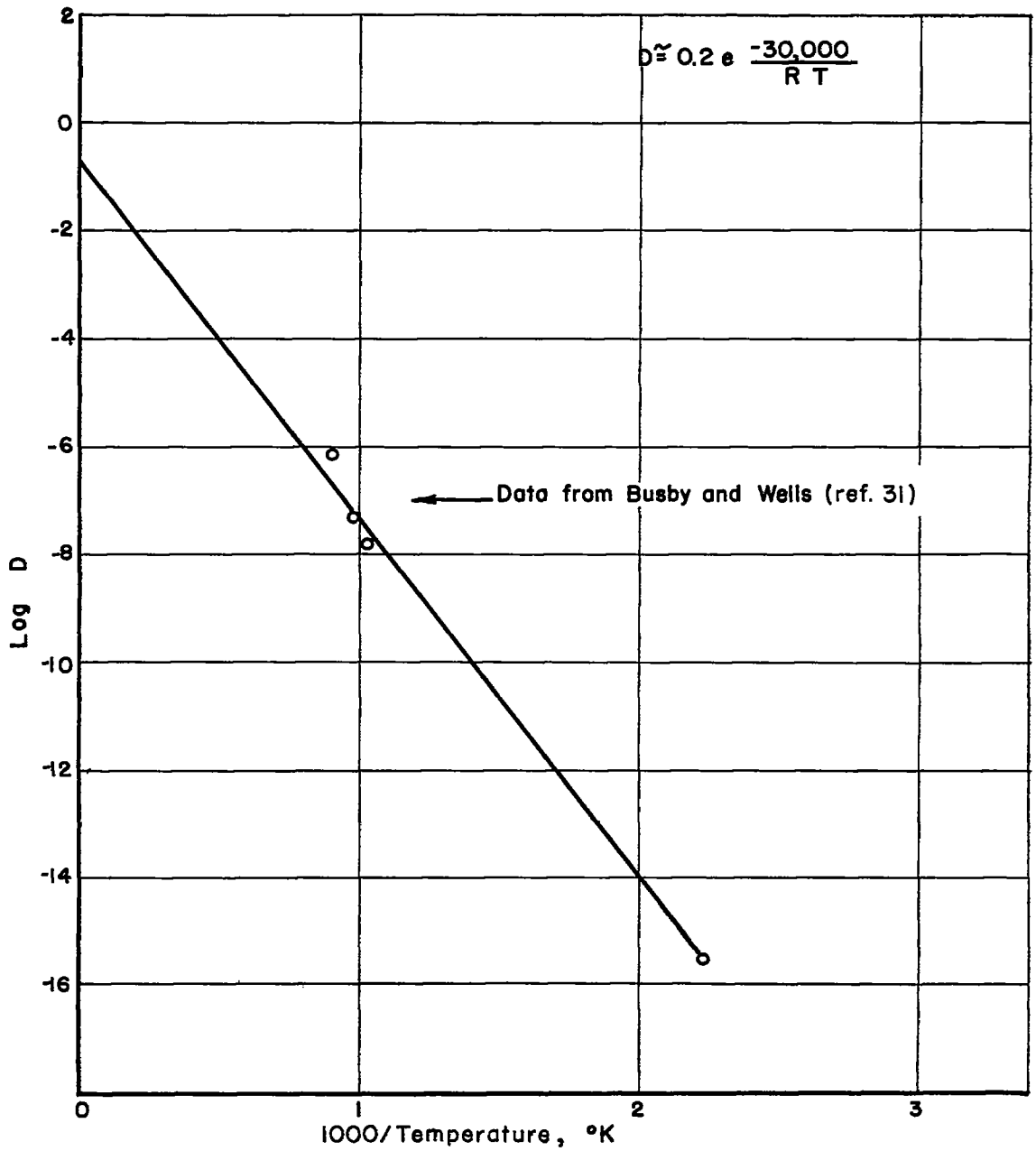

Figure 35. - Speculative plot of temperature dependence of diffusion of boron in Ferrovac E.